

Response to reviewer #1

We would like to thank the reviewer for his/her fruitful comments that helped to improve our manuscript.

*At various places in the manuscript I would encourage the authors to openly discuss the very small sample sizes and that therefore the presented correlations are rather questionable. Everybody will acknowledge that (perhaps fortunately from the perspective of mankind) the set of available volcanic eruptions is very limited, so discussing this in more detail will do the manuscript no harm.*

We certainly agree with the reviewer. The small sample issue has been already mentioned in the paper but is further emphasized in all relevant parts of the manuscript, especially in the conclusions.

*p.2 l. 20: replace "Final" by "The last"*

The text has been modified accordingly in the revised manuscript.

*p.2 l. 22: Potentially it would be advantageous to state that the classification of a "moderate" event is valid in terms of VEI, but not in terms of economic costs.*

A relevant comment has been added in the introduction.

*p. 4 l.1: Please introduce all abbreviations (SMASH).*

The SMASH abbreviation stands for "Satellite Monitoring of Ash and Sulphur dioxide for the mitigation of aviation Hazards" is explained in Page 4 and SACS-2 in page 3. In the revised manuscript will also be explained in the abstract.

*p. 4 l.14: Is it possible to give either a citation for the AAI or to shortly describe the fundamental principles of its derivation for those readers who are not familiar with this method?*

In the revised paper, two references have been included in the text directly after mentioning AAI. The revised text is: "The volcanic ash retrieval algorithm includes an estimation of the optical depth of an ash layer based on the Absorbing Aerosol Index (AAI) (Herman et al., 1997; Torres et al., 1998) as well as an estimation of the effective ash layer height"

*p. 4 l.17: In fact it is the absorbing AOD which is most dominant in AAI. A high AOD of a non-absorbing aerosol will not at all produce a high AAI. Consequently all AAI results are very sensitive to SSA.*

We agree with the reviewer that the absorbing AOD is most dominant in AAI. The AOD from scattering aerosols would lower the AAI values. AAI results are very sensitive to SSA. In the text, we mentioned that AAI is sensitive to aerosol types, AOT .... The sensitivity of AAI to SSA is included implicitly in the sensitivity of AAI to the aerosol type.

*p. 4 l. 27: What are the parameters of the log-normal distributions?*

The parameters of the bi-mode log-normal size distribution for aerosols are effective radius, effective variance for fine and coarse modes, and the weight of the two modes. In our calculations, we used effective radius of 0.052  $\mu\text{m}$  and effective variance of 1.697  $\mu\text{m}$  for the fine mode, effective radius of 0.67  $\mu\text{m}$  and effective variance of 1.806  $\mu\text{m}$  for the coarse mode. The weight of the fine mode is 0.99565. This information is now included in the revised manuscript.

*p. 4 l. 30: I would suggest to split the section 2.1.2 into two subsections, one for the UOXF algorithm and one for the ULB one.*

In the revised version we split section 2.1.2 in two subsections as suggested by the reviewer.

*p. 5 l. 2: What is the spectral resolution of the Eyja refractive indices? Is there already a publication on these?*

The spectral resolution of these indices is 1  $\text{cm}^{-1}$ . As far as we are aware of, these indices have not been published yet.

*p. 5 l. 3: The Pollack database includes pre-tabulated refractive indices as well as oscillator parameters for modelling these. The pre-tabulated indices have rather coarse spectral resolution (given the resolution of the IASI instrument). Which of the two sets has been used? And if it is the pre-tabulated ones, how has the interpolation to the required IASI channels been done?*

The pre-tabulated values have been used, interpolated using the Piecewise Cubic Hermite Interpolating Polynomial, which is shape preserving.

*p. 5 l. 8: What is the mode radius of the log-normal distributions?*

For the ULB the mode radius was retrieved along with the optical depth (see Moxnes et al, 2014). Mode radius is retrieved together with ash optical depth, plume altitude and surface temperature for the Oxford algorithm.

*p. 5 l. 20: Which meteorological input has been used for the RTTOV calculations? Moreover, to my understanding RTTOV is a radiative transfer model, which provides radiance or brightness temperatures or parameters like that which are simulated from given inputs including meteorology, AOD, PSD and such things. So these parameters are input to RTTOV and not provided by the model. Or is there something like an "inverse mode" in RTTOV to obtain these parameters from the radiation field? Then RTTOV would be a suitable retrieval method and no further work would be required*

ECMWF data are used as input to RTTOV. The Oxford iterative algorithm is a full optimal estimation retrieval scheme that calls iteratively the forward model. The forward model is based on RTTOV. RTTOV output for a clean atmosphere (containing gas but not cloud or aerosol/ash) is combined with an ash layer using the same scheme as for the Oxford-RAL Retrieval of Aerosol and Cloud (ORAC) algorithm (Thomas et al., 2009a, 2009b).

In the text we have substituted the sentence:

“RTTOV then provides probable values of AOD, effective radius and plume altitude [Ventress et al. 2015].”

with:

“The iterative retrieval scheme then provides probable values of AOD, effective radius and plume altitude [Ventress et al. 2016].”

*p. 7 l. 9: Please introduce all abbreviations (PCASP and CAS).*

PCASP stands for Passive Cavity Aerosol Spectrometer Probe and CAS stands for Cloud and Aerosol Spectrometer. Both have been introduced in the text.

*p. 8 l. 13: Would it be possible to provide the 532nm refractive index for the Eyjafjalla ash? Or is there already a publication on this?*

The refractive index used for Eyjafjalla ash is  $1.572 + i 7.5e-06$  at 530nm. This value is now mentioned in text of the revised manuscript.

*p. 9 l. 19-20: When the authors say "dust" and "Volz", do they really mean two different algorithms, or do they rather mean two different complex refractive indices used as input for the same algorithm? Please clarify.*

We mean two different complex refractive indices used as input for the same algorithm. This is clarified in the revised manuscript.

*p. 9 l. 29: Give the FOV size of the IASI Instrument, not only thin clouds, but also partially cloudy observation could have an effect.*

This is certainly the case for the ULB algorithm. For that reason, there is a strict quality check at the end of the algorithm, based on the retrieved parameters and the fit residual, which removes most of the cloudy observations. For the Oxford algorithm the spectral variability due to clouds is contained within the covariance matrix and, hence, if the cloud is below the ash plume, it should not present a problem. More details can be found in Ventress et al. 2016.

*p. 10 l. 21: To which number does the number of coincidences decrease? Is the calculation of a correlation coefficient still useful then?*

The number of coincidences with EARLINET stations are shown in the legends of Figure 2. For IASI-UOXF are around 18-20 and for IASI ULB are 13. In any case the sample is small for both data sets.

*p. 15 l. 11: Please replace "excellent" by "very good".*

The text has been modified accordingly

*p. 15. l. 17: The same - given the small sample size I would be rather shy about using the term "excellent".*

The text has been modified accordingly.

*Table II and Table III: Is "Amount of data in days" equivalent to "coincidences"? If not, please provide also the latter number.*

No, it is not equivalent. With "amount of data" it is meant the number of days for which satellite retrievals were available. We introduced an additional column with the number of coincidences in the relevant tables. The number of coincidences are already shown in the legends of the plots.

Response to reviewer #2

We would like to thank the reviewer for his/her fruitful comments that helped to improve our manuscript.

*Correlation coefficient is not enough to define the correlation between satellite retrievals and ground based/airborne based measurements. Correlation coefficient is related with the linear regression between the two sets of data which does not follow 1:1 line. A high correlation coefficient alone does not mean that it exists a good fit between the data. An analysis of the residuals is required as well. Please consider a more complete analysis. Draw regression line along 1:1 line and discuss bias, residuals etc.*

The reviewer is right. Additional results from the statistical analysis (mean bias, rms difference, the slope of the regression line) are shown in the tables and discussed. The figures have been modified accordingly in the revised manuscript.

*pp 5 | 17: define TOVS*

TOVS stands for TIROS Operational Vertical Sounder and has been introduced in the text.

*pp 7 | 7: please describe how LR was chosen and its implication on aerosol extinction coefficient*

An extinction-to-backscatter ratio (lidar ratio) of 60sr was used for the inversion of lidar signals; this lidar ratio was determined in such a way as to satisfy the constraints of a molecular signal below and above lofted layers. This has now been specified in the text in section 2.2.2. Please see Marengo et al, 2011 for details.

*pp 7 | 23: what do you mean by "the closest point in space and time"? Please provide numbers*

We consider for each coincidence the closest point in time and space within the colocation criteria shown in Tables II to VII. The colocation criteria define the upper limits, so the true coincidences in time and space are variable but within these limits. This has been explained in more detail in the text.

*pp 7 | 25: when talking about spatial and temporal filtering, do you refer to the lidar data? Also, please describe the technical details of the filtering (e.g. moving average, resolutions etc)*

What we mean here is that first the spatial colocation criteria have been applied to the satellite data and then the temporal ones. The sentence has been corrected accordingly.

*pp 9 | 28-30: talking about cloud contamination in GOME-2A: isn't possible to screen the cloudy events?*

What we mean here is that despite the screening of the cloudy events contamination could still be possible from thin clouds in the satellite retrievals considering the pixel

size compared to the point lidar measurement. The text has been modified accordingly.

*pp 10 | 21: why the number of coincidences decreases?*

The ULB and UOXF algorithms have different criteria for considering a retrieval as successful.

*pp 10 | 22-23: what is the physical meaning of the "ensemble average"(over the total number of coincidences) of AOD (table IV)? I mean relative error would have been useful.*

The tables have been modified to include additional statistics.

*pp 10 | 26: why do you mention the height of 800 hPa while Fig. 2 is based on the height of 600 hPa?*

Table IV shows results also from comparisons of the "fast algorithm" not shown in Figure 2 in order to reduce the number of subfigures. In figure 2 we only show the 600hPa because it shows the best overall agreement relative to the 800hPa and 400hPa estimates. A relevant comment has been added in the revised text.

*pp 11 | 8-9: the same question for the mean of ash plume height?*

The fast algorithm does not provide plume height, it assumes a fixed plume height.

*pp 12 | 2: what do you mean by "the closest point in space"? Between 50 km and 200 km as mentioned earlier?*

Yes, see our response to a previous comment on the colocation criteria.

*pp 13 | 26: what do you mean by "very good agreement"? Please provide  $r^2$ . Why didn't you provide a scatter plot as in the case of EARLINET comparisons?*

The airborne lidar data give a time series of data for each measurement day. As data are not truly coincident (the overpass time being early in the morning and late in the evening whereas flights were near the middle of the day), volcanic plumes have undergone advection between the measurements. Looking at the data as a time series makes it easier to capture differences due to the misplacement of plumes. We do not show correlation coefficients and scatter plots for the aircraft-satellite comparisons because these are not truly coincident and thus the estimated statistics do not show a good correlation. This could be misleading concerning the usefulness of the comparisons and therefore we decided to show and discuss only qualitatively about the spatial consistency between the aircraft and the satellite data.

*pp 13 | 32: Please rephrase "present the validation". As seen by these results, in my opinion, the validation is not satisfactory (based on present results). It is kind of an attempt to validate... How would you define the criteria for validation?*

We modified the text as follows "present a first attempt to validate improved ...". There were no predefined validation criteria, and no specifically designed validation

campaign. Actually in this paper we examine the consistency between the lidar and the satellite data for volcanic ash retrievals. A relevant comment has been added.

*pp 23 12-5: please reformulate. There is no middle panel in Fig 1.*

The figure caption has been corrected accordingly.

*pp 30 Fig. 2: middle plots: why there are 18 cases on the left plot and 20 cases on the right plot? Then the bottom plot has 13 cases? Please explain. I am also surprised by large  $r$  for the middle and lower plots. The data may be correlated but not with respect to 1:1 line. Please comment on this. The last plot in Fig. 2 looks to me very similar with the lower plot on Fig. 3 while they have quite different  $r$ . I know we talk about different quantities in the two figures but the points are spread quite similar.*

The different number of cases depends on the number of successful satellite retrievals within the spatiotemporal criteria applied and is different for each algorithm. A relevant comment has been included in the text. The discussion on the correlation has been improved and the additional statistics have been included in the discussion.

*pp 32 and pp 33: scatter plots as for EARLINET, including statistics ( $r$ ,  $N$ ) will help comparing the results and be consistent in validation criteria*

See previous comment on aircraft-satellite comparisons.

1 **Validation of ash optical depth and layer height retrieved from**  
2 **passive satellite sensors using EARLINET and airborne lidar**  
3 **data: The case of the Eyjafjallajökull eruption.**

4  
5 D. Balis<sup>1</sup>, M. E. Koukoul<sup>1</sup>, N. Siomos<sup>1</sup>, S. Dimopoulos<sup>1</sup>, L. Mona<sup>2</sup>, G. Pappalardo<sup>2</sup>, F. Marengo<sup>3</sup>,  
6 L. Clarisse<sup>4</sup>, L. J. Ventress<sup>5</sup>, E. Carboni<sup>6</sup>, R. G. Grainger<sup>6</sup>, P. Wang<sup>7</sup>, ~~N. L. G. Tilstra<sup>7</sup>, R. van der~~  
7 ~~A<sup>7</sup>, N.~~ Theys<sup>8</sup> and C. Zehner<sup>9</sup>

8  
9 <sup>1</sup>Laboratory of Atmospheric Physics, Aristotle University of Thessaloniki, Greece,  
10 \*Email:balis@auth.gr

11  
12 <sup>2</sup>Consiglio Nazionale delle Ricerche, Istituto di Metodologie per l'Analisi Ambientale (CNR-  
13 IMAA), Tito Scalo, Potenza, Italy

14  
15 <sup>3</sup>Met Office, Exeter, United Kingdom

16  
17 <sup>4</sup>Université Libre de Bruxelles, Brussels, Belgium

18  
19 <sup>5</sup>National Centre for Earth Observation, Atmospheric, Oceanic and Planetary Physics,  
20 University of Oxford, United Kingdom

21  
22 <sup>6</sup>COMET, Atmospheric, Oceanic and Planetary Physics, University of Oxford, United Kingdom

23  
24 <sup>7</sup>Royal Netherlands Meteorological Institute (KNMI), De Bilt, The Netherlands

25  
26 <sup>8</sup>Belgian Institute for Space Aeronomy (IASB-BIRA), Bruxelles, Belgium

27  
28 <sup>9</sup>European Space Agency, ESRIN, Frascati, Italy

29  
30 **Abstract**

31 The vulnerability of the European airspace to volcanic eruptions was brought to the attention  
32 of the public and the scientific community by the 2010 eruptions of the Icelandic volcano  
33 Eyjafjallajökull. As a consequence of this event ash concentration thresholds replaced the  
34 'zero-tolerance to ash' rule, drastically changing the requirements on satellite ash retrievals.  
35 In response to that, ESA funded several projects aiming at creating an optimal *End-to-End*  
36 *System for Volcanic Ash Plume Monitoring and Prediction*. Two of them, namely the SACS-2  
37 and SMASH projects, developed and improved dedicated satellite-derived ash plume and  
38 sulphur dioxide level assessments. ~~These estimates were extensively validated using ground-~~  
39 ~~based and aircraft lidar measurements.~~The validation of volcanic ash levels and height  
40 extracted from the GOME-2 and IASI instruments on board the MetOp-A satellite is presented  
41 in this work. EARLINET lidar measurements are compared to different satellite retrievals for



1 two eruptive episodes in April and May 2010. Comparisons were also made between satellite  
2 retrievals and aircraft lidar data obtained with UK's BAe-146-301 Atmospheric Research  
3 Aircraft (managed by the Facility for Airborne Atmospheric Measurements, FAAM) over the  
4 United Kingdom and the surrounding regions. The validation results are promising for most  
5 satellite products and are within the estimated uncertainties of each of the comparative  
6 datasets, but more collocation scenes ~~are needed~~would be desirable to perform a  
7 comprehensive statistical analysis. The satellite estimates and the validation data sets are  
8 better correlated for high ash optical depth values, with correlation coefficients greater than  
9 0.8. The IASI ~~data~~retrievals show a better ~~consistency~~agreement concerning the ash optical  
10 depth and ash layer height when compared with the ground-based and airborne lidar data.

11

## 12 1. INTRODUCTION

13 The Eyjafjallajökull volcano in Iceland (63.63°N, 19.62°W) erupted on the 14<sup>th</sup> of April 2010  
14 and the ash-loaded plume rose to more than 10 km, deflected to the east by westerly winds  
15 [Stohl et al., 2011]. The plume persisted over central Europe from the 15<sup>th</sup> and the 26<sup>th</sup> of April  
16 2010, ~~mostly over central Europe~~ while occasionally extending to southeast Europe [Emeis et  
17 al., 2011]. New significant eruptions occurred between May 4<sup>th</sup>–9<sup>th</sup> and May 14<sup>th</sup>–19<sup>th</sup> 2010  
18 [Gudmundsson et al., 2010]. The first of these phases mainly influenced Western Europe, from  
19 Great Britain to the Iberian Peninsula, while the second phase influenced central Europe and  
20 the central and eastern Mediterranean on the May 18<sup>th</sup>–22<sup>nd</sup>. ~~Final~~The last observations of  
21 the event were recorded over central Europe on the 25<sup>th</sup> of May [Gudmundsson et al., 2010].  
22 Although the eruption was a moderate one in terms of volcanic explosivity, due to advection  
23 of the volcanic ash plumes, civil aviation was shut down for many days over numerous  
24 European countries [Gertisser., 2010] ~~and thus in terms of economic costs was more severe.~~  
25 This resulted in an urgent demand for reliable model forecasts of the vertical and horizontal  
26 extent of the ash plume, and for complementary measurements that could be used for  
27 nowcasting and forecast verification [Sears et al., 2013]. Following an eruption, Volcanic Ash  
28 Advisory Centres (VAAC) distributed around the globe give instructions to civil aviation in  
29 order avoid potential hazards [e.g. Guffanti et al., 2010]. Considering the large social and  
30 economic impact of any decision, the provided guidelines should be reliable, verifiable and  
31 should use all available scientific information [Zehner, 2010]. During the eruption period the  
32 European Aerosol Research Lidar Network, EARLINET, responded to this demand with  
33 coordinated intensive measurements from ground-based lidar [e.g. Ansmann et al, 2010;

1 2011; Groß et al., 2011; Mona et al., 2012; Papayannis et al., 2012; Perrone et al., 2012;  
2 Navas-Guzman et al., 2013; Pappalardo et al., 2013; Trickl et al., 2013; Wiegner et al., 2012],  
3 initially by providing quick look images and identification of the volcanic ash layers. This  
4 observation campaign provided information on ash height and its vertical extent, as well as  
5 an estimation of the ash load in terms of optical depth and mass concentration. In addition,  
6 there were a number of dedicated airborne campaigns during the eruption that combined  
7 lidar and in-situ measurements of the ash plume [e.g. Marengo et al., 2011; Schumann et al.,  
8 2011; Chazette et al., 2012]. The volcanic plume was observed from a variety of satellite  
9 sensors/instruments such as the Cloud-Aerosol Lidar with Orthogonal Polarization (CALIOP) on  
10 board the CALIPSO satellite [Winker et al., 2012] and a number of passive satellite sensors  
11 either in low Earth orbit, such as GOME-2/MetopA [e.g. Rix et al., 2012], MODIS/Terra & /Aqua  
12 [e.g. Christopher et al., 2012], IASI/MetopA [Carboni et al., 2012], or in geostationary orbit,  
13 such as SEVIRI [e.g. Francis et al., 2012]. The World Meteorological Organization organized an  
14 intercomparison campaign of twenty two satellite-based volcanic ash retrieval algorithms  
15 applied on passive sensors [WMO, 2015]. The intercomparison was based on six selected  
16 volcanic eruptions including Eyjafjallajökull. Validation results showed variable agreement  
17 with lidar data, depending upon the scene conditions.

18 In 2012 the European Space Agency (ESA) initiated the project “Satellite Monitoring of Ash  
19 and Sulphur Dioxide for the mitigation of Aviation Hazards” (SACS-2) to support authorities  
20 and the VAACs during future volcanic events. The project created an optimal end-to-end  
21 system for volcanic ash plume monitoring and prediction [Brenot et al., 2014 and  
22 <http://sacs.aeronomie.be>]. The system is based on improved and dedicated satellite-derived  
23 ash plume and sulphur dioxide products, followed by extensive validation using satellite and  
24 ground-based measurements [Koukouli et al., 2014a; Spinetti et al., 2014]. In this paper, we  
25 present validation results for two satellite sensors, GOME-2/MetOp-A and IASI/MetOp-A,  
26 concerning the volcanic ash optical depth and ash layer height, using ground and aircraft lidar  
27 measurements. The comparisons are restricted to the Eyjafjallajökull eruption period of 2010.  
28 In the first section we provide a short description of the satellite data and then a description  
29 of the ground-based and aircraft lidar data used as a reference for validation. Then we  
30 describe the methodology applied in the comparisons, and the co-location criteria applied. In  
31 the second section, we present the comparison results for the different sensors and  
32 algorithms, separately for the ground-based and aircraft data. Finally, we discuss the results  
33 and summarize our findings.

1

## 2 2. DATA AND METHODOLOGY

### 3 2.1 SATELLITE DATA

4 One of the main tasks of ESA's SACS-2 and SMASH (*Satellite Monitoring of Ash and Sulphur*  
5 *dioxide for the mitigation of aviation Hazards*) projects was to improve and validate the  
6 algorithms for the retrieval of ash optical depth and height, using satellite measurements in  
7 the infrared and UV-Vis from low Earth orbit sensors. These improvements were based on  
8 previous algorithm developments [e.g. de Graaf et al., 2005; Clerbaux et al., 2009; Clarisse et  
9 al., 2010, 2013; Gangale et al., 2010; Carboni et al., 2012; Grainger et al., 2013] In this paper  
10 we use data from GOME-2 and IASI instruments on board the MetOp-A satellite which covered  
11 the whole eruption period of Eyjafjallajökull in 2010. Details of the satellite data are described  
12 below.

#### 13 2.1.1 GOME-2/METOP-A

14 [The Global Ozone Monitoring Experiment-2 \(GOME-2\) is a visible-ultraviolet scanning](#)  
15 [spectrometer featuring 4096 channels and 200 polarisation channels in the 240-790 nm](#)  
16 [spectral range, and featuring a 40x40 km<sup>2</sup> resolution.](#) Data from GOME-2/MetOp-A have been  
17 processed by the Royal Netherlands Meteorological Institute (KNMI). The volcanic ash  
18 retrieval algorithm includes an estimation of the optical depth of an ash layer based on the  
19 Absorbing Aerosol Index (AAI) ([Herman et al., 1997](#); [Torres et al., 1998](#)) as well as an  
20 estimation of the effective ash layer height. The algorithm is based on look-up tables formed  
21 in terms of the ~~absorbing aerosol index (AAI)~~<sub>z</sub>, aerosol height, solar zenith angle (SZA),  
22 ~~view~~<sub>viewing</sub> zenith angle (VZA), and relative azimuth angle (RAZI). The AAI is sensitive to  
23 atmospheric parameters such as aerosol type, aerosol layer height, and aerosol optical depth  
24 (AOD), and to surface height and scattering geometry [de Graaf et al., 2005]. The most  
25 dominant parameters are aerosol optical thickness and aerosol layer height. In general, thick  
26 aerosol layers produce larger AAI values than thin aerosol layers, while high altitude aerosol  
27 layers produce larger AAI values than low lying aerosol layers [Torres et al., 1998; de Graaf et  
28 al., 2005]. If the aerosol type, surface albedo, and geometries (SZA, VZA, RAZI) are known,  
29 aerosol optical thickness can be calculated using the AAI and aerosol height. The ash layer  
30 height is derived using the Fast REtrieval Scheme for Clouds from Oxygen A-band (FRESCO)  
31 algorithm [Wang et al., 2008a]. It has been demonstrated that FRESCO can retrieve volcanic  
32 ash layer height for optically thick ash plumes [Wang et al., 2012]. The retrieved optical  
33 thickness of the ash layer depends on the assumption of aerosol properties used in the look-

1 up tables (LUTs). The volcanic ash particles are assumed to be spherical and have a bi-modal  
2 log-normal size distribution. In our calculations, we used an effective radius of 0.052  $\mu\text{m}$   
3 and effective variance of 1.697  $\mu\text{m}$  for the fine mode, and an effective radius of 0.67  
4  $\mu\text{m}$  and effective variance of 1.806  $\mu\text{m}$  for the coarse mode. The weight of the fine  
5 mode was 0.995. Two different a priori assumptions for the refractive index of strongly  
6 absorbing volcanic ash were tested, indicated later on as DUST and VOLZ [Volz, 1973; Sinyuk  
7 et al., 2003.]

## 8 **2.1.2 IASI/METOP-A**

9 The Infrared Atmospheric Sounding Interferometer (IASI) is an infrared spectrometer  
10 featuring 8461 channels in the 645-2760  $\text{cm}^{-1}$  spectral range, with a spectral resolution of 0.25  
11  $\text{cm}^{-1}$ . Satellite estimates for the ash optical depth and layer height from IASI/Metop-A have  
12 been provided by two institutes, the Université Libre de Bruxelles (ULB) and the University of  
13 Oxford (UOXF).

### 14 **2.1.2.1 ULB algorithm**

15 The dataset provided by the ULB was generated by a LUT-based algorithm described in  
16 Moxnes et al. [2014] using two distinct sets of refractive indices: one set provided by Dr. Dan  
17 Peters [private communication] based on recent measurements of Eyjafjallajökull ash, and the  
18 other set using the basaltic ash refractive index data from Pollack et al, 1973 (referred to as  
19 the *Eyja* and *Pollack* datasets respectively). In this paper we show only estimates based on the  
20 *Eyja* refractive index. The index was available with a spectral resolution of 1  $\text{cm}^{-1}$ . The  
21 algorithm assumes a log-normal particle size distribution with spread 2. The mode radius is  
22 retrieved together with the ash optical depth. For this eruption, the ash plume was assumed  
23 to be centred at 5 km and no attempt was made to retrieve ash plume height.

### 24 **2.1.2.2 UOXF algorithm**

25 The datasets provided by UOXF also assume the *Eyja* refractive index, and ~~both UOXF and ULB~~  
26 ~~algorithms assume a log-normal~~treat similar the particle size distribution ~~with spread 2.~~. The  
27 algorithmic processing of UOXF resulted in four different products: one characterized as the  
28 'iterative' algorithm, which provided ash optical depth and layer height, and three  
29 characterized as the 'fast' algorithm, which provided ash optical depth for three fixed volcanic  
30 ash layer pressures (400 hPa, 600 hPa and 800 hPa). The fast algorithm, based on the method  
31 of Walker et al. [2011], carries out a linear retrieval (least squares fit) of the aerosol optical

1 depth, AOD, assuming a fixed plume altitude and effective radius. The algorithm looks for  
2 departures in the measured spectra from an expected background covariance, created from  
3 previous IASI measurements containing no volcanic ash. The iterative algorithm is a full  
4 optimal estimation retrieval using a forward model based on Radiative Transfer for TOVS,  
5 [\(TIROS Operational Vertical Sounder\)](#), RTTOV, a very fast radiative transfer model for nadir-  
6 viewing passive visible, infrared and microwave satellite radiometers. Clear sky radiances from  
7 RTTOV are combined with an ash layer in a method described in detail by Thomas et al. [2009a;  
8 2009b]. ~~RTTOV~~[The iterative scheme](#) then provides probable values of AOD, effective radius  
9 and plume altitude [Ventress et al. ~~2015~~[2016](#)]. The fast algorithm is used to flag IASI pixels  
10 (assuming an AOD threshold defined by the statistics of the scene) for the presence of volcanic  
11 ash, at which point the iterative retrieval is carried out on the pixel.

## 12 **2.2 LIDAR DATA**

13 The validation of the satellite products used lidar measurements from two sources. The first  
14 was the intensive ground-based lidar measurements from stations that form the European  
15 Research Lidar Network (EARLINET) and the second was the airborne lidar measurements  
16 from the UK's BAe-146-301 Atmospheric Research Aircraft managed by the Facility for  
17 Airborne Atmospheric Measurements (FAAM). ~~The difference between~~[As a matter of fact, the](#)  
18 ~~aircraft Lidar~~[airborne measurements captured larger volcanic ash load than the ground-based](#)  
19 ~~network, and the EARLINET stations in absolute AOD loadings may be significant, but this is~~  
20 ~~explainable.~~[explained by the fact that the former is a moving platform that was tasked with](#)  
21 [overflying the areas with large concentrations.](#) The aircraft flights monitored a large area  
22 affected by the ash cloud ~~with high ash concentrations.~~ Meanwhile, for most of the EARLINET  
23 stations, the volcanic particles atmospheric content was almost half of that observed in the  
24 UK, which was directly downwind from the eruption.

25 In the next section we provide a brief description of the lidar measurements used as reference  
26 data for the validation of the satellite products.

### 27 **2.2.1 EARLINET DATA**

28 [The European Aerosol Research Lidar Network \(EARLINET\) coordinates ground-based lidar](#)  
29 [activities on the European continent since 2000, and holds a comprehensive database of](#)  
30 [European lidar datasets giving information on the horizontal, vertical and temporal](#)  
31 [distribution of aerosols on a continental scale.](#) Lidar data from the EARLINET network  
32 [Pappalardo et al., 2014 and <http://www.earlinet.org>] were used to validate ash plume height

1 and optical depth. EARLINET was established in 2000 and is the first aerosol lidar network with  
2 the main goal of providing data for investigating the aerosol distribution on a continental  
3 scale. EARLINET has established certain protocols for the measurements and the quality  
4 control of the systems and the retrieved data, through algorithm [Böckmann et al, 2004,  
5 Pappalardo et al, 2004] and system [Matthias et al., 2004a, Freudenthaler et al., 2010,  
6 Wandinger et al., ~~2015~~2016], intercomparison campaigns. The network currently includes 27  
7 stations distributed over the European continent. The standard products of EARLINET include  
8 aerosol extinction and backscatter profiles. EARLINET data have been widely used for  
9 climatological studies [e.g. Matthias et al., 2004b; Amiridis et al., 2005; Giannakaki et al., 2007]  
10 as well as for monitoring unusual atmospheric events such as desert dust, biomass burning,  
11 pollution episodes, volcanic eruptions and so on. Results have been presented in numerous  
12 publications [e.g. Amiridis et al, 2009; Ansmann et al., 2003; Guerrero-Rascado et al.,  
13 2009; Mamouri et al., 2012; Mattis et al., 2010; Mona et al., 2006; Müller et al., 2007;  
14 Papayannis et al., 2008; Wang et al., 2008b].

15 A relational database, containing the output of the 4-D analysis of EARLINET data related to  
16 the volcanic eruption of 2010, has been set up [Mona et al 2012; Pappalardo et al., 2013] and  
17 is freely available on request at <http://www.earlinet.org>. Information related to the present  
18 study involves aerosol backscatter coefficient profiles for each of the ground-based stations  
19 [The EARLINET publishing group 2000–2010, 2014], as well as a characterization of the  
20 observed layers as pure volcanic or mixed [Pappalardo et al., 2013]. A volcanic aerosol mask  
21 was developed [Mona et al., 2012], which involved aerosol typing, ~~backward-back~~-trajectory  
22 analyses and model outputs, used together with the lidar measurements at 1 hour temporal  
23 resolution. The data included in the EARLINET database captured the whole Eyjafjallajökull  
24 eruptive event over Europe providing geometrical and optical properties of the tropospheric  
25 volcanic cloud. The volcanic cloud persisted over central Europe for the whole period at  
26 heights of between 3 and 8 km, with maximum load observed on the 16<sup>th</sup> of April 2010 over  
27 Hamburg [Pappalardo et al., 2013]. In our study we only used profiles that ~~corresponded~~  
28 ~~to~~were detected as pure volcanic, as these were characterized by the methodology applied in  
29 Pappalardo et al., 2013. The list of stations considered for the validation of the satellite  
30 products is shown in **Table 1**.

### 31 **2.2.2 AIRCRAFT AIRBORNE LIDAR DATA**

32 The satellite products are validated using lidar measurements from six flights by the UK's BAe-  
33 146-301 Atmospheric Research Aircraft over the United Kingdom and the surrounding seas in

Field Code Changed

1 May 2010 [e.g. Marengo et al., 2011; Johnson et al., 2011]. The lidar measurements include  
2 aerosol extinction profiles at 355 nm, which in turn provide plume height and layer optical  
3 depth. Measurements were integrated to a vertical resolution of 45 m and a temporal  
4 resolution of 1 min (corresponding to a typical ~9 km horizontal resolution), and all lidar  
5 profiles have been cloud-screened. An extinction-to-backscatter ratio (lidar ratio) of 60 sr was  
6 used for the inversion of lidar signals; this lidar ratio was determined in such a way as to satisfy  
7 the constraints of a molecular signal below and above lofted layers. In situ observations were  
8 provided by other probes on the aircraft, in particular a three-wavelength nephelometer, a  
9 Passive Cavity Aerosol Spectrometer Probe (PCASP) and PCASPa Cloud and Aerosol  
10 Spectrometer (CAS) optical particle counters; radiative measurements were taken in the  
11 visible and infrared. An example of the available aerosol extinction profiles, along with flight  
12 altitude and flight track is shown in **Figure 1** for the 16<sup>th</sup> of May 2010. The data shown here  
13 will be discussed in more detail in the overview of the comparison results. In this paper we  
14 mainly used lidar data from May 4<sup>th</sup>, 5<sup>th</sup>, 14<sup>th</sup>, 16<sup>th</sup>, 17<sup>th</sup> and 18<sup>th</sup> 2010 flights, when volcanic  
15 ash was detected and satellite data were available. Since the satellite AOD estimates were  
16 given at 550 nm we considered scaling the lidar-determined ash layer optical depth to 550 nm  
17 using an appropriate Angstrom exponent. According to Pappalardo et al. [2013] and based on  
18 EARLINET observations, the Angstrom exponent between 355 and 532 nm ranges between  
19 0.03 and -0.11. So we used an exponent equal to zero, which practically means that the optical  
20 depths to be compared were not scaled.

21

#### 22 2.2.2.1 METHODOLOGY FOR THE EARLINET-SATELLITE COMPARISONS

23 The values of each satellite product have been restricted to an area of variable radius around  
24 each EARLINET station, depending on the satellite. The closest ~~point~~measurement in space  
25 and time has been selected for each overpass, ~~and~~within the limits set by the collocation  
26 criteria shown in Table II. This was compared to the respective layer characterized by  
27 EARLINET as volcanic particles. ~~Spatial filtering is~~First the spatial collocation criteria have been  
28 applied before to satellite data and then the temporal filtering ones. The EARLINET relational  
29 database for this event contains cases for which two or more volcanic layers are  
30 simultaneously observed in the atmospheric column. For these cases the worst correlated  
31 layer to the satellite data was excluded from analysis. A summary of the satellite data  
32 compared with the EARLINET measurements and the corresponding collocation criteria can  
33 be found in **Table II**. For all the satellite products a comparison of the AOD has taken place.

1 For the satellite products that provided volcanic ash layer height information a comparison of  
2 volcanic ash layer height was also performed. The AOD of the EARLINET layers was derived by  
3 the layers' integrated backscatter coefficient multiplied by a fixed extinction-to-backscatter  
4 ratio with a value of  $50 \text{ sr}^{-1}$  [Ansmann et al., 2010]. We did not use any Raman lidar  
5 measurements since most comparisons were performed for daytime conditions. An estimated  
6 20% uncertainty on the EARLINET AOD was applied due to the variability of the lidar ratio for  
7 volcanic particles, typically between 40 and  $60 \text{ sr}^{-1}$  [see Pappalardo et al., 2013 and references  
8 therein]. For the layer height comparison, the height of the centre of mass provided by the  
9 EARLINET database was used, and as estimated layer depth, the distance between the mass  
10 centre from the layer top and base was employed. All the satellite ash optical depth products  
11 were calculated at 550 nm, apart from the KNMI/GOME2 products which were calculated first  
12 at 380 nm and then scaled to 550 nm using appropriate Angstrom exponents provided by the  
13 satellite team. In order to convert the infrared optical depth to optical depth at 550 nm, both  
14 ULB and UOXF teams used the Eyja refractive indices from Dr. Dan Peters (private  
15 communication), with a value of  $1.572+i7.5 \cdot 10^{-6}$  at 530nm. Correspondingly, 532 nm lidar  
16 measurements were used in the comparisons.

#### 17 2.2.2.2 METHODOLOGY FOR THE AIRCRAFT-SATELLITE COMPARISONS

18 The airborne lidar data were available on a per flight basis [Koukouli et al., 2014b] and  
19 included aerosol extinction profiles that provided ash plume height and ash layer optical  
20 depth. The values of these variables were compared with the satellite produced values of ash  
21 optical depth and aerosol layer height (where given) ~~over-examining different collocation~~  
22 criteria corresponding to an area of ~~variable~~ radius ranging from 50 km to 200 km ~~(see Table~~  
23 III). The closest satellite value ~~in terms of, within the selected~~ spatial ~~proximity~~ criteria, for  
24 every flight path location was found and ~~presented~~ used for the comparisons. Since the  
25 overpass times of the satellite data are around 9:30 L.T. and 21:30 L.T., in order to allow for  
26 co-location, only spatial criteria were used. None of the available aircraft data were available  
27 within 1-2 hours of the overpass time, which was the criterion that provided the best matches  
28 when using the EARLINET data. The time difference between satellite and aircraft data was  
29 around 5 hours. This fact does not allow a point-to-point comparison of the measurements  
30 but the comparisons will mainly highlight whether the ash products from the two measuring  
31 systems are consistent. A summary of the satellite data compared against the flight  
32 measurements and the corresponding collocation criteria can be found in **Table III**.

33



### 3. RESULTS AND DISCUSSION

#### 3.1 COMPARISON OF ASH OPTICAL DEPTH AND ASH LAYER HEIGHT WITH EARLINET DATA

As shown in **Table III**, we applied different collocation criteria between the EARLINET lidar measurements and the satellite observations, to investigate which one provides the best results and a reasonable number of matches. Although during April and May 2010 the EARLINET stations performed a large number of dedicated intensive measurements, the overpass time of the MetOP-A satellite significantly limited the number of collocations. We examined, for each of the collocation criteria, the correlation coefficient between the lidar-determined optical depth of the pure volcanic particles layer and the corresponding satellite estimate. Furthermore, we examined the correlation coefficient between the ash layer height estimated from the lidar measurements and the one retrieved from the satellite algorithms when available [Koukouli et al., 2014b]. In Figure 2 we present scatter plots between EARLINET ash layer optical depth and each satellite ash product for those collocation criteria that showed the largest correlation. The best correlations were found when limiting the matches to within a radius of 100 km from the ground-based lidar and considering measurements with a one-hour difference. When deviating from these criteria, the number of matches increased but the correlation declined. This fact provides an indication of the spatial and temporal representativeness of single lidar profiles. Different colours in these plots correspond to different European regions (see **Table I**) in order to examine whether the distance from the source and the transport path have an impact on the comparisons.

The GOME-2A comparisons are shown in ~~the~~ Figure 2a and 2b with the "dust" ~~algorithm~~ refractive index in the left column and the "Volz" ~~algorithm~~ refractive index in the right column. Only twelve collocations were found for the GOME-2 and the EARLINET observations. There is a small correlation between the datasets, ranging between 0.33 and 0.46 for the "dust" and "Volz" products respectively. This limited number of co-locations were given by a radius of 300 km from each ground-based station and within 5 hours. The GOME-2A estimates of the ash layer optical depth are systematically larger than the lidar ones and most of them are larger than 1, although for these cases the lidar data rarely exceed the value 0.5. The large GOME-2 pixel size (80 km x 40 km) and the large search radius (300 km) could partly explain differences with point measurements, like the lidar; however it seems possible that ~~many GOME-2A data are contaminated by~~ despite the screening of the cloudy events contamination could still be possible from thin clouds, ~~while the~~ in the GOME-2A retrievals, considering the pixel size, which is compared to the point lidar measurement. The lidar data

1 included in the EARLINET database are always have been thoroughly cloud screened. Between  
2 the two GOME-2A products the “Volz” algorithm shows a slightly better correlation coefficient  
3 with the ground-based lidars.

4 The scatter plots of UOXF ash optical depth and collocated EARLINET measurements are  
5 presented in Figure 2c and 2d; the plot in the left column corresponds to the iterative  
6 algorithm and the right column corresponds to the “fast” algorithm at a fixed height of 600  
7 hPa, which is consistent with the average height where EARLINET observed volcanic particles.  
8 For both algorithms the collocation criteria that provided the best results were a distance from  
9 each ground-based station of 100 km and a maximum time difference of one hour. These  
10 criteria allowed for almost 20 coincidences. As it can be quickly verified by the results shown  
11 in Figure 2c and 2d, the ash AOD extracted from the IASI/MetOpA Oxford iterative algorithm  
12 is quite low, with values rarely rising above 0.2, which is consistent with the EARLINET  
13 measurements, which show similar AOD levels. There are only two cases showing AOD values  
14 larger than 0.2 and these are also consistent with EARLINET, since the lidar data for these two  
15 cases show significantly larger values, above 0.4. The correlation coefficient is quite promising  
16 at 0.85, however it is based on only 18 coincident measurements. The agreement between  
17 IASI and EARLINET estimates is similar for the “fast” algorithm, showing a larger scatter for  
18 the low AOD values but potentially less scatter for larger AODs. This larger scatter leads to a  
19 smaller correlation coefficient close to 0.78. If we loosen the collocation criteria to 300 km  
20 and 3 hours then the correlation coefficient drops significantly to a value of less than 0.5.

21 In Figure 2e we show comparisons of the ash optical depth from the ULB algorithm with  
22 EARLINET estimates. The results are shown for the same collocation criteria applied to UOXF  
23 comparisons, i.e. 100 km distance and one hour difference between the observations. The  
24 general picture is consistent with the IASI/UOXF datasets, however the number of  
25 coincidences decreases to only 13, since the two algorithms have different criteria for  
26 considering a retrieval as successful. The comparisons show a correlation of 0.91, which is  
27 the largest found in all comparisons shown in Figure 2, based however on a small number of  
28 measurements. **Table IV** provides the mean EARLINET and satellite ash optical depths for the  
29 coincidences shown in Figure 2, along with the mean bias, the rms of the differences, the  
30 correlation coefficient and the slope and intercept of the regression line. The average AOD  
31 values of the measurements that meet the collocation criteria are small (less than 0.2) and  
32 consistent with each other, showing a small mean bias, except in the case of GOME-2A and  
33 when the IASI-UOXF fast algorithm has a fixed height of 800 hPa, (not shown in Figure 2).

1 where the satellite data overestimate significantly the ash optical depth. However as it is  
2 demonstrated in the rms differences the scatter is quite large and even when the correlation  
3 coefficients are good, the slope of the regression line is not close to one. Concerning the IASI  
4 retrievals all data sets tend to slightly overestimate the small AOD values and underestimate  
5 the high AOD values, while the GOME-2 as said show a systematic overestimation. We have  
6 to repeat however that all the mean-valuesstatistics are based on a small number of  
7 coincidences.

8 The GOME-2A ash products and the iterative IASI product processed by UOXF provided the  
9 height of the ash layer. These heights were compared with the estimates from EARLINET and  
10 the results are shown in **Figure 3**. The ash plume height estimated for GOME-2A products and  
11 the EARLINET network are compared in Figure 3a. Irrespective of the product and the search  
12 radius (not shown here) the comparison is not satisfactory for either of the two algorithms.  
13 The ~~satellite~~GOME-2A-provided height seems to strongly under-estimate the ground-based  
14 values, showing a ~~very narrow~~narrower range of values between 1 and 25 km. The ground  
15 instruments show a more physical spread of the ash cloud locating it between 32 and 6 km.  
16 The comparison of the ash plume height extracted from the IASI/MetopA UOXF iterative  
17 algorithm and the one observed by the EARLINET network is shown in **Figure 3b**. It is evident  
18 from this figure that the spread of plume heights found by the EARLINET network is higher  
19 than those found by the Oxford iterative IASI algorithm leading to rather poor correlations.  
20 The estimate of the mean is consistent between the datasets. This fact is demonstrated in the  
21 summary **Table V** which gives the mean EARLINET and satellite ash plume height estimates.  
22 The large scatter bars indicate the variability inherent in both sets of observations. We have  
23 to note here that the UOXF-fast algorithm with fixed heights for the ash performs better for  
24 600 hPa, which is consistent with the average heights estimated by the nominal algorithm and  
25 the EARLINET data, which range between 3 and 4 km. In all lidar-satellite comparisons there  
26 was no indication that there were regions where the agreement between the two datasets is  
27 better, due to their proximity to the source. However this conclusion is based, especially for  
28 certain regions, on extremely few data.

### 30 **3.2 COMPARISONS OF ASH OPTICAL DEPTH AND ASH LAYER** 31 **HEIGHT WITH AIRBORNE LIDAR DATA**

32 During May 2010 there were 12 flights of the UK's BAe-146-301 Atmospheric Research Aircraft  
33 [Marenco et al., 2011], and during six of these volcanic ash was detected in the airborne lidar

1 measurements. In order to avoid contamination from cirrus clouds and mixed aerosol layers,  
2 we only show comparisons with the satellite data for two flights, during which significant  
3 levels of pure ash, not mixed with other aerosol types, were observed by the airborne lidar  
4 measurements. The flight that took place on the 16<sup>th</sup> of May 2010 (see also Figure 1), started  
5 at 12:55 U.T. and ended at 18:00 U.T. and the aircraft mostly flew over Scotland and northern  
6 England. During this flight most of the ash was observed between 55° and 56°N. The flight  
7 that took place on the 17<sup>th</sup> of May over the Irish and North Sea, started a little earlier at 11:15  
8 U.T. and ended at 16:58 U.T., and most of the ash was observed over the North Sea between  
9 1° and 2°E. As is demonstrated in **Table III**, we only used spatial criteria to find coincidences  
10 between the airborne lidar data and the satellite data of the same day, since both flights were  
11 performed in the afternoon, while the satellite overpasses are close to 9:30 U.T. (GOME-2A  
12 and IASI) and 21:30 U.T. (IASI only). For GOME-2 we found coincidences only for the 17<sup>th</sup> of  
13 May 2010. The airborne lidar data give a time series of data for each measurement day. As  
14 data are not truly coincident with the satellite data (the overpass time being early in the  
15 morning and late in the evening whereas flights were near the middle of the day), volcanic  
16 plumes have undergone advection between the measurements compared. Looking at the  
17 data as a time series it makes it easier to capture differences due to the misplacement of  
18 plumes. Therefore we do not show correlation coefficients and scatter plots for the satellite-  
19 aircraft comparisons, because these are not truly coincident and thus the estimated statistics  
20 did not show a good correlation. This however could be misleading concerning the usefulness  
21 of the comparisons and therefore we decided to show and discuss only qualitatively about the  
22 spatial consistency between the aircraft and the satellite data.

23

Formatted: English (United States)

24 In **Figure 4** we show the comparisons of the satellite ash optical depth and the airborne lidar  
25 ash layer optical depth for 550 nm as a function of aircraft time (closest point in space). We  
26 also show in the bottom row of **Figure 4** (4e and 4f) the flight track for the two flights  
27 examined. On the path the actual flight time is indicated, in order to be able to identify the  
28 spatial location that corresponds to the footprint of the lidar data. Since the time difference  
29 between the flight measurement and the satellite overpass is large what we would actually  
30 see from the comparisons is (a) if the aircraft and the satellite observe the plume over the  
31 same area and (b) if they observe similar optical depth values. This would occur if the  
32 dispersion, or transport, of the plume was not significant during the hours elapsing between  
33 the satellite overpass and the aircraft measurement, within the spatial criteria we applied for

1 the comparisons. In the **Figure 4a** and **4b** we show the comparisons between IASI ash optical  
2 depth for the iterative and fast algorithm of UOXF versus the ash layer optical depth from the  
3 airborne lidar measurements for the 16<sup>th</sup> of May 2010, where the measurements are shown  
4 as function of time in U.T.C. In **Figure 4e** and **4f**, we plot the flight path for the two days (16  
5 and 17 May 2010). Along the path the flight time in U.T.C is posted, while the different colours  
6 along the flight path indicate the ash optical depth. As we can see, the satellite data processed  
7 with the iterative UOXF algorithm captures the high AODs observed around 14:00 U.T. and  
8 between 16:00 and 17:00 U.T. quite well, ~~but fails to capture~~which is not the case with the  
9 peak observed between 15:00 and 16:00 U.T. Such discrepancies can be expected, considering  
10 the time difference between the airborne data and the satellite measurements. In addition, it  
11 seems that the background is similar but that some larger values are observed between the  
12 ash peaks. The situation is slightly different when examining the comparisons between the  
13 aircraft data and the estimates from the UOXF fast algorithm using a fixed height of the ash  
14 layer at 600 hPa. In general, the UOXF fast algorithm estimates smaller values (including the  
15 background); it captures well the peak observed around 14:00 U.T., overestimates the peak  
16 in AOD observed between 15:00 and 16:00 U.T. and it is hard to tell if the smaller peak  
17 observed around 17:00 U.T. is well-depicted or not.

18 In **Figure 4c**, we present the comparisons between the aircraft data and the estimates from  
19 the ULB-Eyja algorithm again for the 16<sup>th</sup> of May 2010. The satellite estimates follow quite  
20 well all peaks observed in the aircraft data, however slightly misplaced. Checking the SEVIRI  
21 ash imagery at <http://fred.nilu.no> for the 16<sup>th</sup> of May 2010 we observe an almost constant  
22 west-east flow of dust throughout the day between 55°N and 58° N, and thus this plume was  
23 captured both by the morning and by the evening orbit of IASI, as well as by the aircraft when  
24 flying over these latitudes between 14:00 and 16:00 UT. SEVIRI observed a plume after 17:00  
25 UT south of 54° N moving southeast. The early evolution of this plume was captured by the  
26 aircraft around 17:00 and its later evolution was captured over the same area by the evening  
27 orbit of IASI. This plume evolution can partly explain the displacement observed, since the  
28 satellite data are not coincident in time with the aircraft data and the time in x-axis of the  
29 plots actually corresponds to different latitude/longitude of the comparisons.

30 In **Figure 4d** we present the corresponding comparisons between the aircraft data and the  
31 estimates from the GOME-2 KNMI algorithm for the 17<sup>th</sup> of May 2010, and in the right hand  
32 column of the last row of Figure 4 the corresponding flight path of the aircraft. The GOME-2  
33 results capture the levels of the two AOD peaks observed in the aircraft measurements but

Field Code Changed

1 fail to capture small scale variability in the AOD and the background levels. As on 17<sup>th</sup> May  
2 the aircraft mainly flew an East-West track (whereas on the 16<sup>th</sup> it was mainly a North-South  
3 track), the comparison is coarser and the same satellite data point is assigned to several  
4 airborne measurements, resulting in the horizontal lines in Figure 4d. In these cases we  
5 actually compare only the morning orbit (9:30 UT) since GOME-2 is a UV/Vis sensor. SEVIRI  
6 images show a southeast movement of the ash plume starting east of the coast of England  
7 and going towards the Netherlands. The east-west motion of the aircraft over the sea  
8 captured this plume between 14:30 and 15:00, and GOME-2 observed this plume over the  
9 same area in the morning. Before 14:30 UT the aircraft was flying over land and did not  
10 observe any significant ash, so when compared with the morning observations of GOME-2 and  
11 considering the pixel size of GOME-2 and the collocation criteria applied, these measurements  
12 are actually compared with satellite data over the sea. Considering the large time difference  
13 between the flight and GOME-2 overpass and the much larger pixel size of GOME-2, compared  
14 to IASI, it is remarkable that the satellite data can quantitatively capture the ash optical depth  
15 in the greater flight area. **Table VI** summarizes the mean AODs values observed from the  
16 aircraft lidar and each of the satellite products examined.

17 Finally, in **Figure 5** we present the comparisons of the ash layer height observed from the  
18 aircraft measurements and the corresponding effective ash height estimated from the UOXF-  
19 iterative algorithm based on IASI (Figure 5a) and the KNMI algorithm based on GOME-2 (Figure  
20 5b). Considering the constraints induced by the collocation criteria, both algorithms show very  
21 good agreement with the corresponding heights estimated from the airborne lidar data in  
22 most of the collocations, with the ash height mainly ranging between 3 and 5 km. **Table VII**  
23 summarizes the mean ash layer height observed from the aircraft measurements and each  
24 satellite product examined.

25

#### 26 **4. SUMMARY AND CONCLUSIONS**

27 The main aim of this work is to present ~~the validation of a first attempt to validate~~ improved  
28 and dedicated satellite-derived ash plume level assessments as part of the European Space  
29 Agency initiatives, in order to create an optimal “*End-to-End System for Volcanic Ash Plume*  
30 *Monitoring and Prediction systems*”. The data used as reference for the validation were not  
31 part of a specifically designed validation campaign, which explains the small number of  
32 coincident data found. The results shown are complementary to other satellite volcanic ash  
33 products, e.g. from SEVIRI (Prata and Prata, 2012, Clarisse and Prata, 2015, WMO, 2015).

1 Different aerosol optical depth and ash plume height estimations from GOME2/MetopA and  
2 IASI/MetopA have been assessed against collocated ground-based and airborne Lidar data for  
3 the 2010 eruptions of the Icelandic volcano Eyjafjallajökull. The GOME2/MetopA  
4 measurements have been analysed by the Royal Netherlands Meteorological Institute (KNMI)  
5 and the IASI/MetopA observations by both the Université Libre de Bruxelles (ULB) and the  
6 University of Oxford (UOXF). Different algorithm versions and parameters were examined and  
7 inter-compared. Both aerosol optical depth and ash plume height satellite estimates were  
8 compared with European Aerosol Research Lidar Network [EARLINET] lidar measurements  
9 and the UK's BAe-146-301 Atmospheric Research Aircraft flying over the UK during the  
10 eruptive period.

11 ▪ The KNMI GOME2 AOD over-estimates the ground-based values, showing quite high  
12 values for cases where the LIDAR sees a low AOD. As a result, the *dust* algorithm shows  
13 relatively low correlation coefficients of between 0.25 and 0.3 depending on the  
14 spatiotemporal search radius, whereas the *Volz* algorithms perform slightly better, with  
15  $r^2$  values ranging between 0.4 and 0.5. The KNMI/GOME2 data seem to suffer from the  
16 spatial resolution of the satellite instrument which made the spatial criterion rather too  
17 large hence precluding any conclusive comparisons when compared to the aircraft  
18 measurements. The agreement between the satellite-derived and airborne lidar effective  
19 ash heights differ only by 1 km on the average, indicating a homogenous spread of the  
20 plume under the satellite's pixel. The KNMI GOME2 ash plume height comparisons are  
21 not satisfactory, irrespective of the search radius, for either of the two algorithms. The  
22 satellite ash height values seem to under-estimate the ground-based values, having a very  
23 narrow range of values between 1 and 2 km and a mean of  $2.07 \pm 1.22$  km. In comparisons,  
24 the ground instruments show a more natural spread between 3 and 6 km with a mean of  
25  $3.92 \pm 1.22$  km. It is highly likely that the large GOME-2 pixel size smooths out any small  
26 scale variability of the plume height, otherwise captured by the ground-based single point  
27 measurements.

28 ▪ The Oxford nominal IASI algorithm shows satisfactory AOD correlations against the  
29 ground AODs, with coefficients ranging between 0.6 and 0.85, and, even though it  
30 provides rather small optical depths, these are of the same order of magnitude as the  
31 lidar. The algorithm presents quite good comparisons for the AOD patterns observed with  
32 aircraft lidar. The Oxford nominal IASI algorithm ash plume height comparisons do not  
33 show any significant correlation with the EARLINET estimates. The satellite estimates have  
34 no spread in values compared to the lidar estimates, however both datasets show similar

1 average values, indicating that the satellite estimates can capture the average conditions.  
2 The results are better when compared with the aircraft lidar, where it seems that the  
3 satellite estimates follow the variability of ash height along the flight route; however they  
4 slightly underestimate the height values with a mean of  $3.73 \pm 1.45$  km [compared to the  
5 aircraft mean of  $4.30 \pm 2.00$  km].

- 6 ▪ The Oxford fast IASI algorithm also provides the same order of magnitude AOD estimates  
7 as the ground lidar, with the narrower spatio-temporal choice providing the most  
8 promising results: the 400 hPa product has a correlation of around 0.7 and the 800 hPa  
9 product a correlation of around 0.8. The Oxford fast IASI algorithm shows ~~an excellent~~  
10 very good agreement with the aircraft lidar, where the 600 hPa product, that corresponds  
11 to the actual plume height, appears to perform best.
- 12 ▪ The ULB AOD estimates are the most promising, showing the highest correlation  
13 coefficients, ranging between 0.74 and 0.91, depending on the spatio-temporal criterion  
14 chosen. This is also valid when we examine the ULB IASI – aircraft comparisons. The ULB  
15 IASI algorithm shows ~~excellent~~ very good agreement, both with respect to the absolute  
16 AOD values and with AOD features during the flight shown. The actual absolute AOD  
17 maxima are also represented best by this product.

18  
19 Concluding, we note that, depending on the careful choice of collocation criteria, the satellite  
20 algorithms investigated here can observe the ash optical depth and plume height for large  
21 enough eruptions to a satisfactory degree. The results shown in this study are in line with the  
22 main finding of the dedicated WMO intercomparison study [2015] concerning the agreement  
23 between satellite ash products and validation data sets (for AOD correlations between 0.4 and  
24 0.6 and ash layer height agreement within 2km) and in some cases the results shown here  
25 show better statistics. However, in order to quantify the levels of accuracy of the satellite  
26 assessments, eruptions with strong ash plumes need to be included in this type of validation  
27 exercise, since there were too few co-location scenes for most satellite products for the  
28 Eyjafjallajökull and Grimsvötn 2010 and 2011 eruptions, as examined in the course of the  
29 SACS/SMASH ESA projects. This validation study highlights the need for dedicated validation  
30 campaigns during volcanic eruptions. For future eruptions it could be recommended to fly  
31 instrumented aircraft along the satellite orbit in order to optimize the collocations between  
32 satellite data and aircraft-based observations. It is recognised however that this would be a  
33 difficult campaign to plan, given that it is not possible to make ~~precise~~ long-term predictions  
34 of the eruptions.



1

## 2 **Acknowledgements**

3 The comparison study was funded by the European Space Agency in the frame of the “Satellite  
4 Monitoring of Ash and Sulphur dioxide for the mitigation of Aviation Hazards”-SACS-2 project.  
5 The financial support for EARLINET in the ACTRIS Research Infrastructure Project by the  
6 European Union’s Horizon 2020 research and innovation program under grant agreement n.  
7 654169 and previously under grant agreement n. 262254 in the 7thFramework Program  
8 (FP7/2007-2013) is gratefully acknowledged. The UK’s BAe-146-301 Atmospheric Research  
9 Aircraft flown by Directflight Ltd and managed by the Facility for Airborne Atmospheric  
10 Measurements (FAAM), which a joint entity of the Natural Environment Research Council  
11 (NERC) and the Met Office. L.C. is a research associate with the Belgian F.R.S.-FNRS. LJV was  
12 funded through the NERC National Centre for Earth Observation. RGG and EC were supported  
13 by the NERC Centre for Observation and Modelling of Earthquakes, Volcanoes, and Tectonics  
14 (COMET).

15

16

17

## 1 References

- 2 Ansmann, A., et al., (2003), Long-range transport of Saharan dust to northern Europe: The 11-  
3 16 October 2001 outbreak with EARLINET, *Journal of Geophysical Research*, 108, 4783, doi:  
4 10.1029/2003JD003757.
- 5 Ansmann, A., et al. (2010), The 16 April 2010 major volcanic ash plume over central Europe:  
6 EARLINET lidar and AERONET photometer observations at Leipzig and Munich, Germany,  
7 *Geophys. Res. Lett.*, 37, L13810, doi:10.1029/2010GL043809.
- 8 Ansmann, A., et al. (2011), Ash and fine-mode particle mass profiles from EARLINET-AERONET  
9 observations over central Europe after the eruptions of the Eyjafjallajökull volcano in 2010,  
10 *J. Geophys. Res.*, 116, D00U02, doi:10.1029/2010JD015567.
- 11 Amiridis V., D. Balis, S. Kazadzis, A. Bais, E. Giannakaki, A. Papayannis and C. Zerefos, (2005),  
12 Four years aerosol observations with a Raman lidar at Thessaloniki, Greece in the  
13 framework of EARLINET, *J. Geophys. Res.*, Vol. 110, D21203, doi:10.1029/2005JD006190.
- 14 Amiridis, V., Balis, D. S., Giannakaki, E., Stohl, A., Kazadzis, S., Koukouli, M. E., and Zanis, P.,  
15 (2009), Optical characteristics of biomass burning aerosols over Southeastern Europe  
16 determined from UV-Raman lidar measurements, *Atmos. Chem. Phys.*, 9, 2431-2440,  
17 doi:10.5194/acp-9-2431-2009.
- 18 Brenot, H., et al., (2014), Support to Aviation Control Service (SACS): an online service for near-  
19 real-time satellite monitoring of volcanic plumes, *Nat. Hazards Earth Syst. Sci.*, 14, 1099-  
20 1123, doi:10.5194/nhess-14-1099-2014.
- 21 Böckmann, C., U. Wandinger, A. Ansmann, et al., (2004), Aerosol lidar intercomparison in the  
22 framework of EARLINET: Part II-Aerosol backscatter algorithms, *Applied Optics* 43, 977-  
23 989.
- 24 Carboni, E., Grainger, R., Walker, J., Dudhia, A., and Siddans, R. (2012), A new scheme for  
25 sulphur dioxide retrieval from IASI measurements: application to the Eyjafjallajökull  
26 eruption of April and May 2010, *Atmos. Chem. Phys.*, 12, 11417-11434, doi:10.5194/acp-  
27 12-11417-2012.
- 28 [Chazette, P., Dabas, A., Sanak, J., Lardier, M., and Royer, P.: French airborne lidar](#)  
29 [measurements for Eyjafjallajökull ash plume survey, \*Atmos. Chem. Phys.\*, 12, 7059-7072,](#)  
30 [doi:10.5194/acp-12-7059-2012, 2012.](#)
- 31 Christopher, S. A., N. Feng, A. Naeger, B. Johnson, and F. Marengo (2012), Satellite remote  
32 sensing analysis of the 2010 Eyjafjallajökull volcanic ash cloud over the North Sea during  
33 4–18 May 2010, *J. Geophys. Res.*, 117, D00U20, doi:10.1029/2011JD016850.
- 34 Clarisse, L., Hurtmans, D., Prata, A. J., Karagulian, F., Clerbaux, C., Mazière, M. D. and Coheur,  
35 P.-F., (2010), Retrieving radius, concentration, optical depth, and mass of different types  
36 of aerosols from high-resolution infrared nadir spectra, *Appl. Opt.*, 49, 3713-3722, doi:  
37 10.1364/AO.49.003713.
- 38 Clarisse, L., Coheur, P.-F., Prata, F., et al., (2013), A unified approach to infrared aerosol  
39 remote sensing and type specification, *Atmos. Chem. Phys.*, 13, 2195-2221,  
40 doi:10.5194/acp-13-2195-2013.
- 41 Clarisse, L and F. Prata (2015), Infrared sounding of volcanic ash, in *Volcanic Ash: Methods of*  
42 *observation and monitoring* (eds S. Mackie, K. Cashman, A. Rust, H. Ricketts and I.M.  
43 Watson), in press

1 Clerbaux, C., Boynard, A., Clarisse, L., et al., (2009), Monitoring of atmospheric composition  
 2 using the thermal infrared IASI/MetOp sounder, *Atmos. Chem. Phys.*, 9, 6041-6054,  
 3 doi:10.5194/acp-9-6041-2009.

4 Gangale, G., A. J. Prata, and L. Clarisse (2010), The infrared spectral signature of volcanic ash  
 5 determined from high spectral resolution satellite measurements, *Remote Sens.*  
 6 *Environ.*, 114, 414–425, 10.1016/j.rse.2009.09.007.

7 ~~The EARLINET publishing group 2000 2010, Adam, M., Alados Arboledas, L., Althausen, D.,~~  
 8 ~~Amiridis, V., Amodeo, A., Ansmann, A., Apituley, A., Arshinov, Y., Balis, D., Belegante,~~  
 9 ~~L., Bobrovnikov, S., Boselli, A., Bravo Aranda, J. A., Bösenberg, J., Carstea, E., Chaikovskiy, A.,~~  
 10 ~~Comerón, A., D’Amico, G., Daou, D., Dreischuh, T., Engelmann, R., Finger, F.,~~  
 11 ~~Freudenthaler, V., García Vázquez, D., García, A. J. F., Geiß, A., Giannakaki, E., Giehl, H.,~~  
 12 ~~Giunta, A., de Graaf, M., Granados Muñoz, M. J., Grein, M., Grigorev, I., Groß, S., Gruening,~~  
 13 ~~C., Guerrero Rascado, J. L., Haeffelin, M., Hayek, T., Iarlori, M., Kanitz, T., Kokkalis, P., Linné,~~  
 14 ~~H., Madonna, F., Mamouriat, R. E., Matthias, V., Mattis, I., Menéndez, F. M., Mitev,~~  
 15 ~~V., Mona, L., Morille, Y., Muñoz, C., Müller, A., Müller, D., Navas Guzmán, F., Nemeš, A.,~~  
 16 ~~Nicolae, D., Pandolfi, M., Papayannis, A., Pappalardo, G., Pelon, J., Perrone, M. R.,~~  
 17 ~~Pietruczuk, A., Pisani, G., Potma, C., Preißler, J., Pujadas, M., Putaud, J., Radu, C., Ravetta,~~  
 18 ~~F., Reigert, A., Rizi, V., Rocadenbosch, F., Rodríguez, A., Sauvage, L., Schmidt, J., Schnell, F.,~~  
 19 ~~Schwarz, A., Seifert, P., Serikov, I., Sicard, M., Silva, A. M., Simeonov, V., Siomos, N., Sirch,~~  
 20 ~~T., Spinelli, N., Stoyanov, D., Talianu, C., Tesche, M., De Tomasi, F., Trickl, T., Vaughan, G.,~~  
 21 ~~Volten, H., Wagner, F., Wandinger, U., Wang, X., Wiegner, M., and Wilson, K. M.: EARLINET~~  
 22 ~~observations related to volcanic eruptions (2000–2010), *World Data Center for Climate*~~  
 23 ~~(WDCC), doi:10.1594/WDCC/EN\_VolcanicEruption\_2000-2010\_2014.~~

24

25 Giannakaki, E., Balis, D. S., Amiridis, V., and Kazadzis, S., (2007), Optical and geometrical  
 26 characteristics of cirrus clouds over a Southern European lidar station, *Atmos. Chem. Phys.*,  
 27 7, 5519-5530, doi:10.5194/acp-7-5519-2007.

28 de Graaf, M., P. Stammes, O. Torres, and R. B. A. Koelemeijer (2005), Absorbing Aerosol Index:  
 29 Sensitivity analysis, application to GOME and comparison with TOMS, *J. Geophys. Res.*,  
 30 110, D01201, doi:10.1029/2004JD005178.

31 Grainger, R. G., D. M. Peters, G. E. Thomas, A. Smith, R. Siddans, E. Carboni, and A. Dudhia  
 32 (2013), Measuring volcanic plume and ash properties from space, in *remote sensing of*  
 33 *volcanoes and volcanic processes: Integrating observation and modelling, Geol. Soc. Spec.*  
 34 *Publ.*, 380, doi:10.1144/SP380.7.

35 Emeis, S., Forkel, R., Junkermann, W., Schäfer, K., Flentje, H., Gilge, S., Fricke, W.,  
 36 Wiegner, M., Freudenthaler, V., Groß, S., Ries, L., Meinhardt, F., Birmili, W., Münkel, C.,  
 37 Obleitner, F., and Suppan, P.: Measurement and simulation of the 16/17 April 2010  
 38 Eyjafjallajökull volcanic ash layer dispersion in the northern Alpine region, *Atmos. Chem.*  
 39 *Phys.*, 11, 2689-2701, doi:10.5194/acp-11-2689-2011, 2011.

40 Francis, P. N., M. C. Cooke, and R. W. Saunders (2012), Retrieval of physical properties of  
 41 volcanic ash using Meteosat: A case study from the 2010 Eyjafjallajökull eruption, *J.*  
 42 *Geophys. Res.*, 117, D00U09, doi:10.1029/2011JD016788.

43 Freudenthaler, V., et al., (2010), EARLI09 – direct intercomparison of eleven EARLINET lidar  
 44 systems, in: *Proceedings of the 25th International Laser Radar Conference, St. Petersburg,*  
 45 *Russia, 5–9 July, 891–894.*

46 Gertisser R., (2010), Eyjafjallajökull causes widespread disruption to European air traffic, *Geol.*  
 47 *Today*, 26, 94-95

Field Code Changed

1 Groß, S., V. Freudenthaler, M. Wiegner, J. Gasteiger, A. Geiß, and F. Schnell (2011), Dual-  
2 wavelength linear depolarization ratio of volcanic aerosols: lidar measurements of the  
3 Eyjafjallajökull plume over Maisach, Germany, *Atmos. Environ.*, 48, 85-96, doi:  
4 10.1016/j.atmosenv.2011.06.017.

5 Gudmundsson, M. T., R. Pedersen, K. Vogfjörð, B. Thorbjarnardóttir, S. Jakobsdóttir, and M. J.  
6 Roberts (2010), Eruptions of Eyjafjallajökull Volcano, Iceland, *Eos Trans. AGU*, 91(21), 190-  
7 191, doi:[10.1029/2010EO210002](https://doi.org/10.1029/2010EO210002).

8 Guerrero-Rascado, J. L., Olmo, F. J., Avilés-Rodríguez, I., Navas-Guzmán, F., Pérez-Ramírez, D.,  
9 Lyamani, H., and Alados Arboledas, L., (2009), Extreme Saharan dust event over the  
10 southern Iberian Peninsula in September 2007: active and passive remote sensing from  
11 surface and satellite, *Atmos. Chem. Phys.*, 9, 8453-8469, doi:10.5194/acp-9-8453-2009.

12 Guffanti M., D.J. Schneider, K.L. Wallace, T. Hall, D.R. Bensimon and L.J. Salinas (2010),  
13 Aviation response to widely dispersed volcanic ash and gas cloud from the August 2008  
14 eruption of Kasatochi, Alaska, USA, *J. Geophys. Res.*, 115, D00L19,  
15 doi:10.1029/2010JD013868.

16 ~~Herman, J. R., Bhartia, P. K., Torres, O., Hsu, C., Seftor, C., and Celarier, E., (1997), Global~~  
17 ~~distributions of UV-absorbing aerosols from Nimbus 7/TOMS data, *J. Geophys. Res.*,~~  
18 ~~102(D14), 16,911–16,922, doi:10.1029/96JD03680~~

19 Johnson, B., et al. (2012), In situ observations of volcanic ash clouds from the FAAM aircraft  
20 during the eruption of Eyjafjallajökull in 2010, *J. Geophys. Res.*, 117, D00U24,  
21 doi:10.1029/2011JD016760

22 ~~Emeis, S., Forkel, R., Junkermann, W., Schäfer, K., Flentje, H., Gilge, S., Fricke, W.,~~  
23 ~~Wiegner, M., Freudenthaler, V., Groß, S., Ries, L., Meinhardt, F., Birmili, W., Münkler, C.,~~  
24 ~~Obleitner, F., and Suppan, P., Measurement and simulation of the 16/17 April 2010~~  
25 ~~Eyjafjallajökull volcanic ash layer dispersion in the northern Alpine region, *Atmos. Chem.*~~  
26 ~~*Phys.*, 11, 2689–2701, doi:10.5194/acp-11-2689-2011, 2011.~~

27 ~~Francis, P. N., M. C. Cooke, and R. W. Saunders (2012), Retrieval of physical properties of~~  
28 ~~volcanic ash using Meteosat: A case study from the 2010 Eyjafjallajökull eruption, *J.*~~  
29 ~~*Geophys. Res.*, 117, D00U09, doi:10.1029/2011JD016788.~~

30 ~~Freudenthaler, V., et al., (2010), EARLI09 – direct intercomparison of eleven EARLINET lidar~~  
31 ~~systems, in: Proceedings of the 25th International Laser Radar Conference, St. Petersburg,~~  
32 ~~Russia, 5–9 July, 891–894.~~

33 Koukoulis, M. E., L. Clarisse, E. Carboni, et al., (2014a), Intercomparison of Metop-A SO2  
34 measurements during the 2010-2011 Icelandic eruptions, *Annals in Geophysics*, Vol 57,  
35 Fast Track 2, <http://dx.doi.org/10.4401/ag-6613>.

36 Koukoulis, M. E., et al. (2014b), SACS2/SMASH Validation Report on the Eyjafjallajökull &  
37 Grímsvötn Eruptions, [http://sacs.aeronomie.be/Documentation/LAP-AU.T.H-SACS-](http://sacs.aeronomie.be/Documentation/LAP-AU.T.H-SACS-ValidationReport_FINAL.pdf)  
38 [ValidationReport\\_FINAL.pdf](http://sacs.aeronomie.be/Documentation/LAP-AU.T.H-SACS-ValidationReport_FINAL.pdf), last accessed: Tuesday, April 26, 2016.

39 Levelt P.F., et al., (2006), The Ozone Monitoring Instrument, *IEEE Trans. Geosc. Rem. Sens.*, 44  
40 (5), 1093-1101.

41 ~~Gangale, G., A. J. Prata, and L. Clarisse (2010), The infrared spectral signature of volcanic ash~~  
42 ~~determined from high spectral resolution satellite measurements, *Remote Sens.*~~  
43 ~~*Environ.*, 114, 414–425, doi:10.1016/j.rse.2009.09.007.~~

44 ~~Grainger, R. G., D. M. Peters, G. E. Thomas, A. Smith, R. Siddans, E. Carboni, and A. Dudhia~~  
45 ~~(2013), Measuring volcanic plume and ash properties from space, in remote sensing of~~

Field Code Changed

Field Code Changed

Field Code Changed

1 ~~volcanoes and volcanic processes: Integrating observation and modelling, Geol. Soc. Spec.~~  
2 ~~Publ., 380, doi:10.1144/SP380.7.~~

3 Mamouri, R. E., Papayannis, A., Amiridis, V., Müller, D., Kokkalis, P., Rapsomanikis, S.,  
4 Karageorgos, E. T., Tsaknakis, G., Nenes, A., Kazadzis, S., and Remoundaki, E., (2012), Multi-  
5 wavelength Raman lidar, sun photometric and aircraft measurements in combination with  
6 inversion models for the estimation of the aerosol optical and physico-chemical properties  
7 over Athens, Greece, *Atmos. Meas. Tech.*, 5, 1793-1808, doi:10.5194/amt-5-1793-2012.

8 Matthias V., J. Bösenberg, V. Freudenthaler, A. Amodeo, D. Balis, A. Chaikovsky, G. Chourdakis,  
9 A. Comerón, A. Delaval, F. de Tomasi, R. Eixmann, A. Hågård, L. Komguem, S. Kreipl, R.  
10 Matthey, I. Mattis, V. Rizi, J.A. Rodriguez, V. Simeonov, X. Wang, (2004a), Aerosol lidar  
11 intercomparison in the framework of the EARLINET project. 1. Instruments, *Appl. Opt.* 43,  
12 N. 4, 961-976.

13 Matthias V., D. Balis, J. Bösenberg, R. Eixmann, M. Iarlori, L. Komguem, I. Mattis, A.  
14 Papayannis, G. Pappalardo, M.R. Perrone and X. Wang, (2004b), Vertical aerosol  
15 distribution over Europe: Statistical analysis of Raman lidar data from 10 European Aerosol  
16 Research Lidar Network (EARLINET) stations, *Journal of Geophysical Research-*  
17 *Atmospheres*, 109, D18, D18201.

18 Mattis, I., P. Siefert, D. Müller, M. Tesche, A. Hiebsch, T. Kanitz, J. Schmidt, F. Finger, U.  
19 Wandinger, and A. Ansmann, (2010), Volcanic aerosol layers observed with  
20 multiwavelength Raman lidar over central Europe in 2008–2009, *J. Geophys. Res.*, 115,  
21 D00L04, doi:10.1029/2009JD013472.

22 Marenco F., B. Johnson, K. Turnbull, S. Newman, J. Haywood, H. Webster and H. Ricketts,  
23 (2011), Airborne lidar observations of the 2010 Eyjafjallajökull volcanic ash plume, *J.*  
24 *Geophys. Res.*, 116, D00U05, doi:10.1029/2011JD016396.

25 Mona L., A. Amodeo, M. Pandolfi and G. Pappalardo, (2006), Saharan dust intrusions in the  
26 Mediterranean area: three years of lidar measurements in Potenza, *J. Geophys. Res.*, vol.  
27 111, D16203, doi:10.1029/2005JD006569.

28 Mona, L., A. Amodeo, G. D'Amico, A. Giunta, F. Madonna, and G. Pappalardo, (2012), Multi-  
29 wavelength Raman lidar observations of the Eyjafjallajökull volcanic cloud over Potenza,  
30 Southern Italy, *Atmos. Chem. Phys.*, 12, 2229-2244, doi:10.5194/acp-12-2229-2012.

31 Moxnes, E. D., N. I. Kristiansen, A. Stohl, L. Clarisse, A. Durant, K. Weber, and A. Vogel (2014),  
32 Separation of ash and sulfur dioxide during the 2011 Grímsvötn eruption, *J. Geophys. Res.*  
33 *Atmos.*, 119, 7477–7501, doi:10.1002/2013JD021129.

34 Müller, D., Mattis, I., Ansmann, A., Wandinger, U., Ritter, C., Kaiser, D., (2007),  
35 Multiwavelength Raman lidar observations of particle growth during long-range transport  
36 of forest-fire smoke in the free troposphere. *Geophys. Res. Lett.*, 34, L05803,  
37 2006GL027936.

38 Navas-Guzman, F., D. Müller, J. A. Bravo-Aranda, J. L. Guerrero-Rascado, M. J. Granados-  
39 Munoz, D. Perez-Ramirez, F. J. Olmo, and L. Alados-Arboledas, (2013), Eruption of the  
40 Eyjafjallajökull Volcano in spring 2010: Multiwavelength Raman lidar measurements of  
41 sulphate particles in the lower troposphere. *J. Geophys. Res.*, 118, 1804–1813,  
42 doi:10.1002/jgrd.50116.

43 Pappalardo G., et al., (2004), Aerosol lidar intercomparison in the framework of the EARLINET  
44 project. 3. Raman lidar algorithm for aerosol extinction, backscatter and lidar ratio, *Appl.*  
45 *Opt.*, 43. N. 28, 53705385.

- 1 Pappalardo G., L. Moma, G. D'Amico, et al., (2013) Four-dimensional distribution of the 2010  
2 Eyjafjallajökull volcanic cloud over Europe observed by EARLINET, *Atmos. Chem. Phys.*, 13,  
3 4429-4450, doi:10.5194/acp-13-4429-2013.
- 4 Pappalardo, G., et al., (2014), EARLINET: towards an advanced sustainable European aerosol  
5 lidar network, *Atmos. Meas. Tech.*, 7, 2389-2409, doi:10.5194/amt-7-2389-2014.
- 6 Papayannis A., et al., (2008), Systematic lidar observations of Saharan dust over Europe in the  
7 frame of EARLINET (2000-2002), *Journal of Geophysical Research*, 113,  
8 doi:10.1029/2007JD009028.
- 9 Papayannis, A., et al., (2012), Optical properties and vertical extension of aged ash layers over  
10 the Eastern Mediterranean as observed by Raman lidars during the Eyjafjallajökull eruption  
11 in May 2010, *Atmospheric Environment*, 48, 56-65,  
12 doi:10.1016/j.atmosenv.2011.08.037.
- 13 Perrone, M. R., De Tomasi, F., Stohl, A., and Kristiansen, N. I., (2012), Integration of  
14 measurements and model simulations to characterize Eyjafjallajökull volcanic aerosols  
15 over south-eastern Italy, *Atmos. Chem. Phys.*, 12, 10001-10013, doi:10.5194/acp-12-  
16 10001-2012.
- 17 Pollack, J., Toon, O. and Khare, B., (1973), Optical properties of some terrestrial rocks and  
18 glasses, *Icarus*, 19, 372-389.
- 19 Prata, A.J. and A.T. Prata, (2012), Eyjafjallajökull volcanic ash concentrations determined using  
20 Spin Enhanced Visible and Infrared Imager measurements, *J. Geophys. Res.*, doi:  
21 10.1029/2011JD016800
- 22 Rix, M., P. Valks, N. Hao, D. Loyola, H. Schlager, H. Huntrieser, J. Flemming, U. Koehler, U.  
23 Schumann, and A. Inness, (2012), Volcanic SO<sub>2</sub>, BrO and plume height estimations using  
24 GOME-2 satellite measurements during the eruption of Eyjafjallajökull in May 2010, *J.*  
25 *Geophys. Res.*, 117, D00U19, doi:10.1029/2011JD016718.
- 26 Sears, T. M., G. E. Thomas, E. Carboni, A. J. A. Smith, and R. G. Grainger (2013), SO<sub>2</sub> as a possible  
27 proxy for volcanic ash in aviation hazard avoidance, *J. Geophys. Res. Atmos.*, 118, 5698–  
28 5709, doi:10.1002/jgrd.50505
- 29 Schumann, U., et al., (2011), Airborne observations of the Eyjafjalla volcano ash cloud over  
30 Europe during air space closure in April and May 2010, *Atmos. Chem. Phys.*, 11, 2245-2279,  
31 doi:10.5194/acp-11-2245-2011.
- 32 Sinyuk, A., Torres, O., and Dubovik, O., (2003), Combined use of satellite and surface  
33 observations to infer the imaginary part of refractive index of Saharan dust, *Geophys. Res.*  
34 *Lett.*, 30, 1081, doi:10.1029/2002GL016189.
- 35 Spinetti C, G. Salerno, T. Caltabiano, et al., (2014), Volcanic SO<sub>2</sub> by UV-TIR satellite retrievals:  
36 validation by using ground-based network at Mt. Etna, *Annals in Geophysics*, Vol 57,  
37 <http://dx.doi.org/10.4401/ag-6641>, Fast Track 2.
- 38 Stohl, A., et al., (2011), Determination of time- and height-resolved volcanic ash emissions and  
39 their use for quantitative ash dispersion modeling: the 2010 Eyjafjallajökull eruption,  
40 *Atmos. Chem. Phys.*, 11, 4333-4351, doi:10.5194/acp-11-4333-2011.
- 41 [The EARLINET publishing group 2000-2010, Adam, M., Alados-Arboledas, L., Althausen, D.,](#)  
42 [Amiridis, V., Amodeo, A., Ansmann, A., Apituley, A., Arshinov, Y., Balis, D., Belegante,](#)  
43 [L., Bobrovnikov, S., Boselli, A., Bravo-Aranda, J. A., Bösenberg, J., Carstea, E., Chaikovskiy, A.,](#)  
44 [Comerón, A., D'Amico, G., Daou, D., Dreischuh, T., Engelmann, R., Finger, F.,](#)  
45 [Freudenthaler, V., Garcia-Vizcaino, D., García, A. J. F., Geiß, A., Giannakaki, E., Giehl, H.,](#)  
46 [Giunta, A., de Graaf, M., Granados-Muñoz, M. J., Grein, M., Grigorov, I., Groß, S., Gruening,](#)

- 1 [C.,Guerrero-Rascado, J. L., Haeffelin, M., Hayek, T., Iarlori, M., Kanitz, T., Kokkalis, P., Linné,](#)  
2 [H., Madonna, F., Mamouriat, R.-E., Matthias, V., Mattis, I., Menéndez, F. M., Mitev,](#)  
3 [V., Mona, L., Morille, Y., Muñoz, C., Müller, A., Müller, D., Navas-Guzmán, F., Nemuc, A.,](#)  
4 [Nicolae, D., Pandolfi, M., Papayannis, A., Pappalardo, G., Pelon, J., Perrone, M. R.,](#)  
5 [Pietruczuk, A., Pisani, G., Potma, C., Preißler, J., Pujadas, M., Putaud, J., Radu, C., Ravetta,](#)  
6 [F., Reigert, A., Rizi, V., Rocadenbosch, F., Rodríguez, A., Sauvage, L., Schmidt, J., Schnell, F.,](#)  
7 [Schwarz, A., Seifert, P., Serikov, I., Sicard, M., Silva, A. M., Simeonov, V., Siomos, N., Sirch,](#)  
8 [T., Spinelli, N., Stoyanov, D., Talianu, C., Tesche, M., De Tomasi, F., Trickl, T., Vaughan, G.,](#)  
9 [Volten, H., Wagner, F., Wandinger, U., Wang, X., Wiegner, M., and Wilson, K. M.: EARLINET](#)  
10 [observations related to volcanic eruptions \(2000–2010\), World Data Center for Climate](#)  
11 [\(WDCC\), doi:10.1594/WDCC/EN\\_VolcanicEruption\\_2000-2010, 2014.](#)
- 12 Thomas, G. E., Poulsen, C. A., Sayer, A. M., Marsh, S. H., Dean, S. M., Carboni, E., Siddans, R.,  
13 Grainger, R. G. and Lawrence, B. N., (2009a), The GRAPE aerosol retrieval algorithm,  
14 *Atmos. Meas. Tech.*, 2, 679-701, doi:10.5194/amt-2-679-2009.
- 15 Thomas, G. E., E. Carboni, A.M. Sayer, et al., (2009b), Oxford-RAL Aerosol and Cloud (ORAC):  
16 aerosol retrievals from satellite radiometers in Satellite Aerosol Remote Sensing Over Land  
17 (Eds: A.A. Kokhanovsky and G. de Leeuw), Springer.
- 18 Torres, O., Bhartia, P. K., Herman, J. R., Ahmad, Z., and Gleason, J., (1998), Derivation of  
19 aerosol properties from satellite measurements of backscattered ultraviolet radiation:  
20 theoretical basis, *J. Geophys. Res.*, 103, D14, <http://dx.doi.org/10.1029/98JD00900>.
- 21 [Trickl T., H. Giehl, H. Jaeger, and H. Vogelmann, 35 years of stratospheric aerosol](#)  
22 [measurements at Garmisch-Partenkirchen: from Fuego to Eyjafjallajökull, and beyond,](#)  
23 [\(2013\), Atmos. Chem. Phys., 13, 5205–5225, doi:10.5194/acp-13-5205-2013](#)
- 24 Ventress, L.J.; Carboni, E.; Grainger, R.G.; Smith, A. J. Retrieval of ash optical properties from  
25 IASI measurements. *Atmos. Chem. Phys.* in prep. (2016)
- 26 Volz, F. E., (2973), Infrared optical constants of ammonium sulfate, Sahara dust, volcanic  
27 pumice and fly ash, *Appl. Opt.* 12,564-568.
- 28 Walker, J. C., Dudhia, A., and Carboni, E., (2011), An effective method for the detection of  
29 trace species demonstrated using the MetOp Infrared Atmospheric Sounding  
30 Interferometer, *Atmos. Meas. Tech.*, 4, 1567-1580, doi:10.5194/amt-4-1567-2011.
- 31 Wang, P., Stammes, P., van der A, R., Pinaridi, G., and van Roozendael, M., (2008a), FRESKO+:  
32 an improved O2 A-band cloud retrieval algorithm for tropospheric trace gas retrievals,  
33 *Atmos. Chem. Phys.*, 8, 6565-6576, <http://dx.doi.org/10.5194/acp-8-6565-2008>.
- 34 Wang, P., O. N.E. Tuinder, L. G. Tilstra, M. de Graaf and P. Stammes, (2012), Interpretation of  
35 FRESKO cloud retrievals in case of absorbing aerosol events, *Atm. Chem. Phys.*,  
36 doi:10.5194/acp-12-9057-2012.
- 37 Wang X., A. Boselli, L. D'Avino, G. Pisani, N. Spinelli, A. Amodeo, A. Chaikovsky, M. Wiegner, S.  
38 Nickovic, A. Papayannis, M.R. Perrone, V. Rizi, L. Sauvage and A. Stohl, (2008b), Volcanic  
39 dust characterization by EARLINET during Etna's eruptions in 2001-2002, *Atmospheric*  
40 *Environment* ,42, 893–905.
- 41 Wandinger, U., et al., (2015,2016), EARLINET instrument intercomparison campaigns:  
42 overview on strategy and results, *Atmos. Meas. Tech. Discuss.*, 8, 10473–10522, 9, 1001-  
43 1023, doi:10.5194/amt-8-10473-2015,amt-9-1001-2016.
- 44 [Wiegner, M., J. Gasteiger, S. Groß, F. Schnell, V. Freudenthaler, and R. Forkel \(2012\),](#)  
45 [Characterization of the Eyjafjallajökull ash-plume: Potential of lidar remote sensing,](#)  
46 [Physics and Chemistry of the Earth 45-46 \(2012\) 79-86, doi: 10.1016/j.pce.2011.01.006.](#)

Field Code Changed

Formatted: Default Paragraph Font, Font color: Black, English (United States)

1

2 Winker, D. M., Z. Liu, A. Omar, J. Tackett, and D. Fairlie (2012), CALIOP observations of the  
3 transport of ash from the Eyjafjallajökull volcano in April 2010, *J. Geophys. Res.*, 117,  
4 D00U15, doi:10.1029/2011JD016499.

5 World Meteorological Organization (2015) WMO SCOPE-Nowcasting: Meeting on the  
6 Intercomparison of Satellite based Volcanic Ash Retrieval Algorithms, Final Report,  
7 [http://www.wmo.int/pages/prog/sat/documents/SCOPE-NWC-](http://www.wmo.int/pages/prog/sat/documents/SCOPE-NWC-PP2_VAIntercompWSReport2015.pdf)  
8 [PP2\\_VAIntercompWSReport2015.pdf](http://www.wmo.int/pages/prog/sat/documents/SCOPE-NWC-PP2_VAIntercompWSReport2015.pdf), last accessed 2/12/2015

Field Code Changed

9 Zehner C., Ed. (2010). Monitoring Volcanic Ash from Space. Proceedings of the ESA-EUMETSAT  
10 workshop on the 14 April to 23 May 2010 eruption at the Eyjafjoll volcano, South Iceland.  
11 Frascati, Italy, 26-27 May 2010. ESA-Publication STM-280. doi:10.5270/atmch-10-01.

12



1 **Figure captions**

2 Figure 1. Characteristics of the FAAM flight of 16-5-2010. The flight track ~~colored~~coloured with  
3 AOD (a), and the flight altitude versus time in UT along with a time-altitude cross section for  
4 the aerosol extinction coefficient at 355nm (in  $Mm^{-1}$ ) measured with the aircraft lidar (b).

5 Figure 2. Scatter plots between satellite ash optical depth at 550nm and EARLINET ash layer  
6 optical depth at 532nm for GOME-2A (a) and (b), IASI-UOXF (c) and (d) and IASI-ULB (e)  
7 products. Different colors correspond to different European domains. See Table I for more  
8 details.

9 Figure 3. Scatter plots between satellite ash layer height and EARLINET ash layer height (in  
10 km), for GOME-2A (a), and IASI-UOXF (b).

11 Figure 4. Ash optical depth at 550nm and airborne lidar ash layer optical depth at 355 nm as  
12 a function of aircraft time. IASI-UOXF products for the 16<sup>th</sup> of May 2010 (a) and (b), IASI-ULB  
13 products for the 16<sup>th</sup> of May 2010 (c) and GOME-2A product for the 17<sup>th</sup> of May 2010 (d). The  
14 flight tracks for these two days, colored with AOD are shown in (e) and (f)

15 Figure 5. Ash layer height and aircraft lidar ash layer height (in km) 355nm as a function of  
16 aircraft time,. GOME-2A for 17<sup>th</sup> of May 2010 (a), and IASI-UOXF for the 16<sup>th</sup> of May 2010 (b).

17

18

1 **Table I.** Locations of EARLINET lidar stations, their geographical coordinates and corresponding domain  
 2 assigned (C: Central Europe, N: North-Central Europe, SW: Iberian Peninsula, SE: Italy-Balkans).

Site	Altitude a.s.l. (m)	Lat. (N)	Long. (E)	Domain
Andøya, Norway	380	69.28	16.01	N
Athens, Greece	200	37.96	23.78	SE
Barcelona, Spain	115	41.39	2.11	SW
Belsk, Poland	180	51.84	20.79	N
Bucharest-Magurele, Romania	93	44.45	26.03	SE
Cabauw, The Netherlands	1	51.97	4.93	N
Evora, Portugal				SW
Garmisch-Partenkirchen, Germany	730	47.48	11.06	C
Granada, Spain	680	37.16	-3.61	SW
Hamburg, Germany	25	53.57	9.97	N
Ispra, Italy	209	45.82	8.63	C
L'Aquila, Italy	683	42.38	13.32	SE
Lecce, Italy	30	40.30	18.10	SE
Leipzig, Germany	100	51.35	12.44	N
Linköping, Sweden	80	58.39	15.57	N
Madrid, Spain	669	40.45	-3.73	SW
Maisach, Germany	515	48.21	11.26	C
Minsk, Belarus	200	53.92	27.60	N
Napoli, Italy	118	40.84	14.18	SE
Neuchâtel, Switzerland	487	47.00	6.96	C
OHP, France	683	43.96	5.71	SW
Palaiseau, France	162	48.70	2.20	N
Payerne, Switzerland	456	46.81	6.94	C
Potenza, Italy	760	40.60	15.72	SE
Sofia, Bulgaria	550	42.67	23.33	SE
Thessaloniki, Greece	60	40.63	22.95	SE

3

1 **Table II.** Collocation criteria examined in the EARLINET-satellite comparisons

Institute	Satellite product	Overpass time	Amount of Data In days	Co-location Criteria	<u>Number of coincidences</u>	Comments
KNMI	GOME2/MetopA	09:30 LT	14	3h & 300km <del>5h &amp; 300km</del> 3h & 500km <del>5h &amp; 500km</del>	<u>12</u>	
UOXF	IASI/MetopA-Nominal Algorithm	09:30 LT 21:30 LT	18	1h & 100km <del>3h &amp; 300km</del>	<u>18</u>	
UOXF	IASI/MetopA-Fast Algorithm	09:30 LT 21:30 LT	19	1h & 100km <del>1h &amp; 300km</del> <del>3h &amp; 100km</del> <del>3h &amp; 300km</del>	<u>20</u>	3 fixed heights provided, 400 hPa, 600 hPa & 800 hPa
ULB	IASI/MetopA	09:30 LT 21:30 LT	48	1h & 100km <del>1h &amp; 300km</del> <del>3h &amp; 100km</del> <del>3h &amp; 300km</del>	<u>13</u>	

Formatted: Centered

Formatted Table

Inserted Cells

Formatted: Centered

Formatted: Centered

Inserted Cells

Formatted: Centered

Formatted: Centered

Formatted: Centered

Inserted Cells

Formatted: Centered

Formatted: Centered

Inserted Cells

2

3

1 **Table III.** Collocation criteria examined in the aircraft-satellite comparisons. The flights were  
 2 performed between 13:00 and 17:30 U.T..

Institute	Satellite product	Overpass time	Amount of data in days	Co-location Criteria	<u>Number of coincidences</u>	Comments
			<b>Max # 5</b>	<b>No time constraint</b>		
KNMI	GOME2/MetopA	09:30 LT	1	100km/200km	<u>64</u>	
UOXF	IASI/MetopA-Nominal Algorithm	09:30 LT 21:30 LT	4	50/100/200km	<u>787</u>	
UOXF	IASI/MetopA-Fast Algorithm	09:30 LT 21:30 LT	4	50/100/200km	<u>732-776</u>	3 fixed heights provided, 400, 600 & 800mbar
ULB	IASI/MetopA	09:30 LT 21:30 LT	5	50/100/200km	<u>463</u>	

Formatted Table

Inserted Cells

Formatted: Centered

Formatted: Centered

Formatted: Centered

Formatted: Centered

Inserted Cells

Formatted: Centered

Inserted Cells

3  
4

1 **Table IV.** Statistical mean values and associated standard deviation for the EARLINET and  
 2 the satellite ash optical depth estimates presented for collocated measurements.

Product	Spatiotemporal criteria	<del>EARLINET mean AOD at 532nm</del>	Satellite mean AOD at 550nm	<del>EARLINET mean AOD at 532nm</del>	Bias (SAT-GB)	RMS difference			
GOME-2A, KNMI dust	300km & 5h		<u>1.18±0.43</u>	<u>0.19±0.2221</u>	<u>1.29±0.4898</u>	<u>0.41</u>			
GOME-2A, KNMI volz	300km & 5h		<u>1.17±0.61</u>	<u>0.19±0.2221</u>	<u>1.32±0.6997</u>	<u>0.55</u>			
IASI, UOXF nominal	100km & 1h		<u>0.08±0.08</u>	0.12±0.12	- <u>0.08±0.0804</u>	<u>0.07</u>	<u>0.85</u>	<u>0.53</u>	<u>0.02</u>
IASI, UOXF fast 400hPa	100km & 1h		<u>0.10±0.04</u>	0.12±0.12	- <u>0.10±0.0401</u>	<u>0.1</u>	<u>0.70</u>	<u>0.21</u>	<u>0.07</u>
IASI, UOXF fast 600hPa	100km & 1h		<u>0.12±0.12</u>	<u>0.12±0.12</u>	<u>0.05</u>	<u>0.08</u>			
IASI, UOXF fast 800 hPa	100km & 1h		<u>0.32±0.38</u>	0.12±0.12	<u>0.32±0.3820</u>	<u>0.28</u>			
IASI, ULB	100km & 1h		<u>0.09±0.07</u>	0.14±0.14	- <u>0.09±0.0704</u>	<u>0.08</u>	<u>0.91</u>	<u>0.43</u>	<u>0.03</u>

3  
 4 **Table V.** Statistical mean values and associated standard deviation for the EARLINET and the  
 5 satellite ash plume height estimates.

Product	Spatiotemporal criteria	<del>EARLINET</del> Satellite mean and standard deviation [km]	Satellite <del>EARLINET</del> mean and standard deviation [km]	Mean Bias (SAT-GB) in km	RMS difference in km			
IASI, UOXF nominal	100km & 1h	<u>3.4±0.78</u>	3.63±0.95	<u>3.4±0.7822</u>	<u>1.39</u>			
GOME2/MetOp-A	300km & 5h	<u>2.07±1.22</u>	3.92±1.22	<u>2.07±1.2284</u>	<u>2.18</u>			

6  
 7

1 **Table VI.** Statistical mean values and associated standard deviation for the airborne lidar  
 2 and the satellite ash optical depth estimates at 550nm presented for collocated  
 3 measurements.

Institute	Instrument & algorithm	Spatial criteria	Mean Satellite AOD levels	Mean Aircraft AOD Levels	Number of common observations (SAT-AIR)	RMS difference
KNMI	GOME-2/MetOp-A	200km	0.42±0.03	0.23±0.15	640.19	0.26
UOXF	IASI/Metop A Nominal Algorithm	50km	0.28±0.25	0.19±0.16	7870.09	0.28
UOXF	IASI/Metop A Fast Algorithm 400hPa	50km	0.20±0.30	0.19±0.16	7760.01	0.29
UOXF	IASI/Metop A Fast Algorithm 600hPa	50km	0.23±0.29	0.18±0.15	7490.05	0.26
UOXF	IASI/Metop A Fast Algorithm 800hPa	50km	0.30±0.40	0.18±0.16	7320.11	0.37
ULB	IASI/Metop A	50km	0.21±0.15	0.25±0.17	4630.04	0.23

Inserted Cells

Inserted Cells

4

5

6 **Table VII.** Statistical mean values and associated standard deviation for the airborne lidar  
 7 and the satellite ash plume height estimates.

Product	Spatial criteria	Aircraft mean and standard deviation [km]	Satellite mean and standard deviation [km]	Bias (SAT-AIR) in km	RMS difference
IASI/MetOpA, UOXF nominal	50km	3.73±1.45	4.30±2.00	-0.59±1.45	2.29
GOME-2-MetOpA, KNMI	200km	5.62±0.54	3.87±1.70	1.75±0.54	2.33

Inserted Cells

Inserted Cells

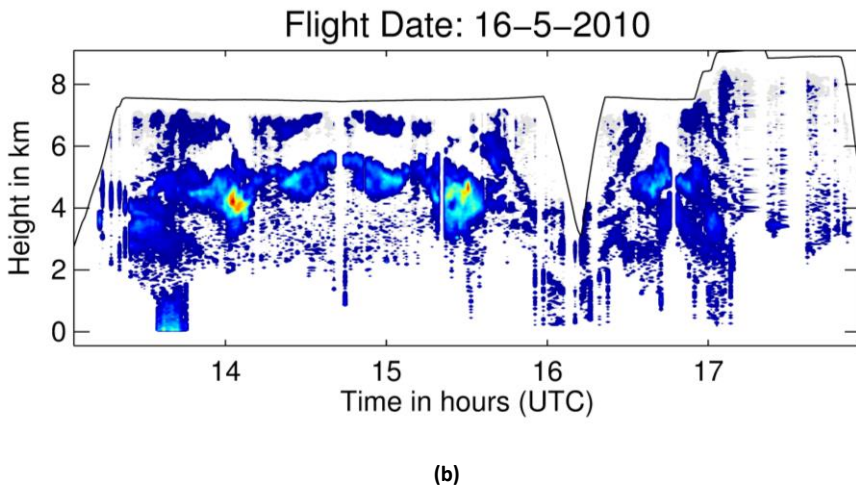
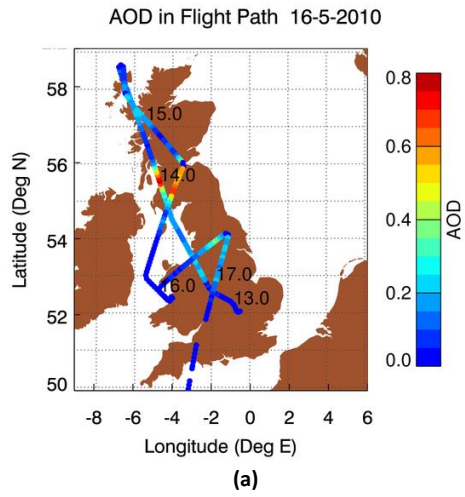
Formatted Table

Inserted Cells

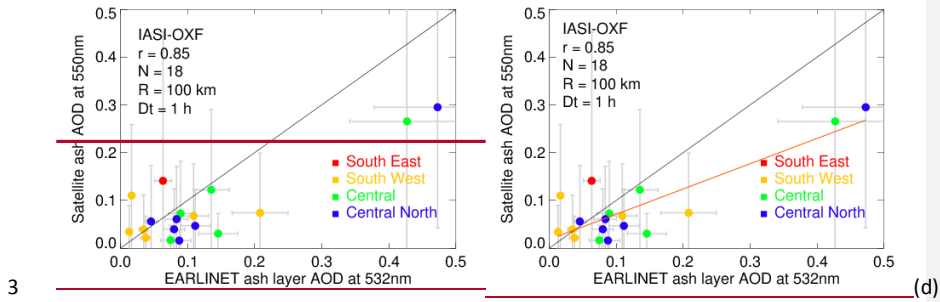
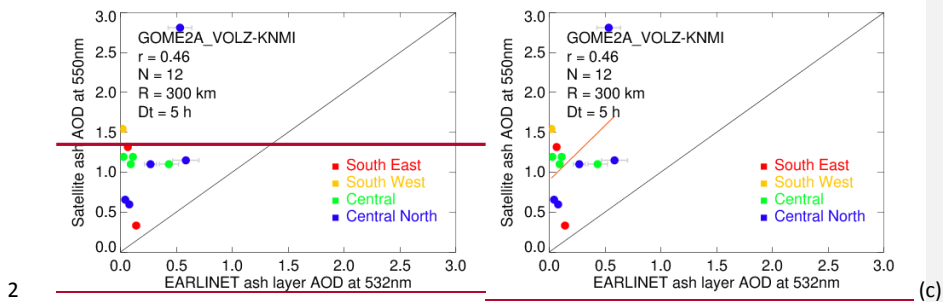
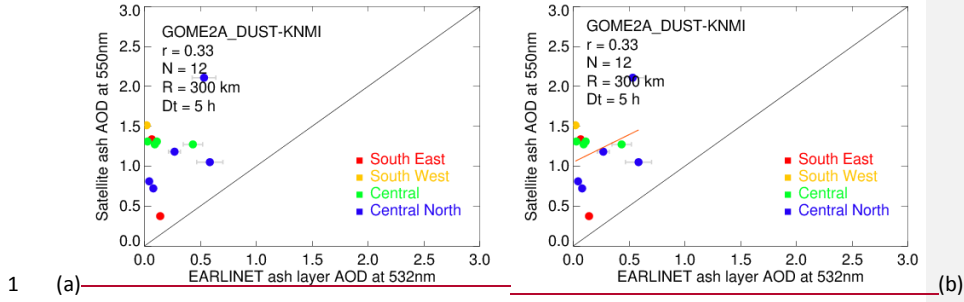
8

9

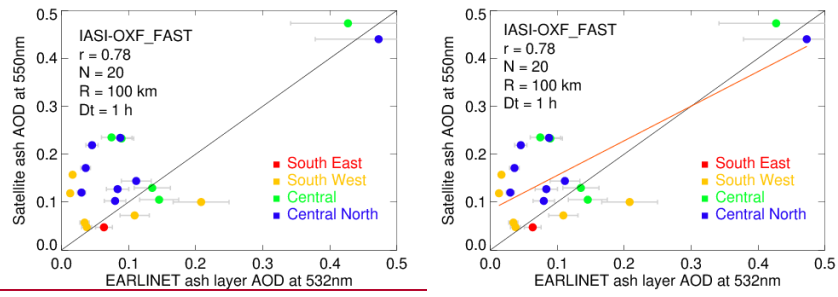
1



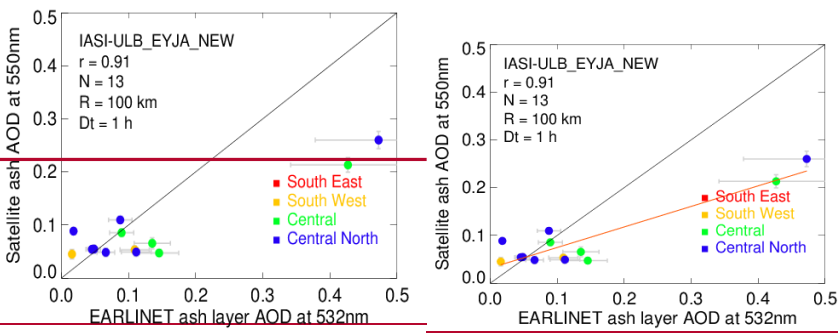
2 Figure 1.







1



2

Figure 2.

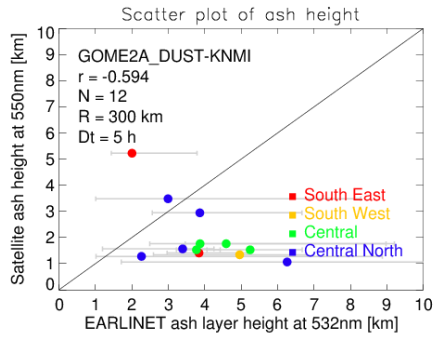
3

4

5

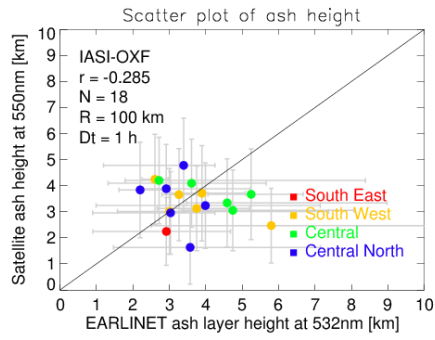
6

1



2

(a)



3

(b)

Figure 3.

4

5

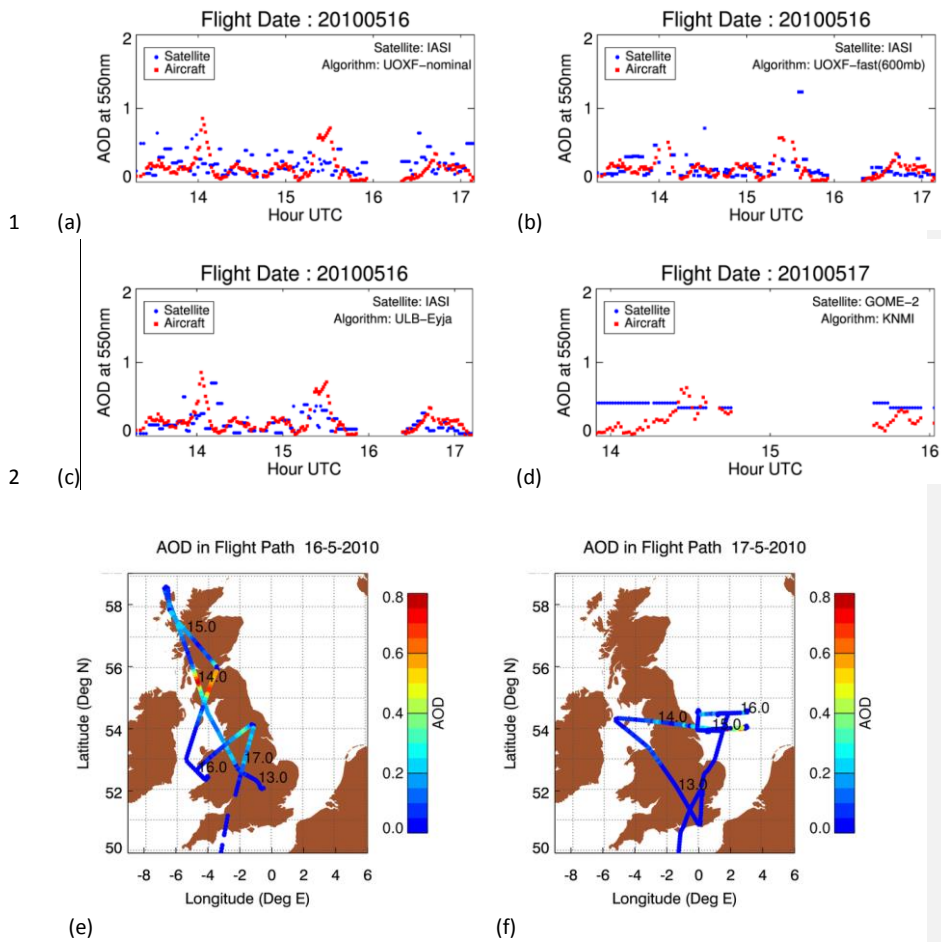
6

7

8

9

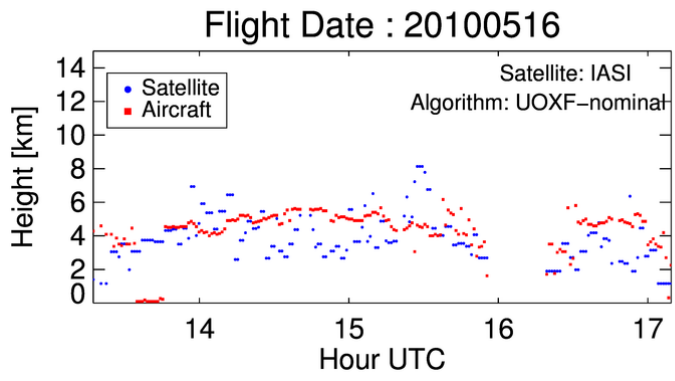
10



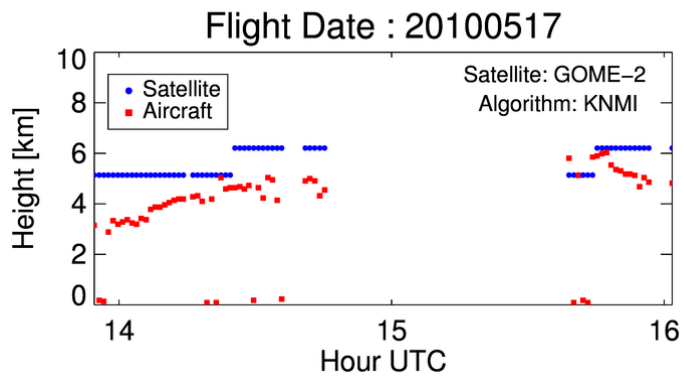
3 **Figure 4.**

4

1



2 (a)



3 (b)

4 **Figure 5.**

5

6

7

8

9

10